the various curves are distinguishable, but their magnitudes are so small that the present experiment could not see them. It is possible, however, that an experiment with highly enriched targets, good resolution, and very low background could observe states having a three-quadrupole-phonon character.

4. SUMMARY

We have measured the scattering of 14.0-MeV protons from the even isotopes of cadmium. Coupled-channel analysis, using optical-model parameters that vary in a reasonable way as a function of neutron excess, provides good fits to the experimental angular distributions. By using values for β_{02} from the compilation of Stelson and Grodzins,[20] we have determined W_D, since the cross section for exciting the first 2^+ state is sensitive to the combination of β_{02} and W_D. The analysis thus yields a value for the imaginary part of the isospin-dependent part of the extended optical model. The analysis indicates that the nuclear radius does not vary as $A^{1/3}$ in the isotopic sequence; appreciable improvement in the quality of the fits, especially those to the one-quadrupole-phonon and one-octupole-phonon states, is achieved when a constant value for the nuclear radius is employed. The octupole state has been identified in each nucleus, and enhancement factors 29 to 40 times single-particle estimates are deduced for these transitions. The second 2^+ state, sometimes thought of as a member of a two-quadrupole-phonon triplet, has some direct coupling to the ground state. Finally, the β values deduced indicate substantial reductions below the vibrational-model prediction for the ratios of the strength of the electric quadrupole transition between a member of the two-quadrupole-phonon triplet and the first 2^+ state to that of the 2^+ state to the ground state.

PHYSICAL REVIEW VOLUME 178, NUMBER 4 20 FEBRUARY 1969

Nuclear Levels in Re^{186}†

R. G. LANIER* AND R. K. SHELINE
The Florida State University, Tallahassee, Florida
AND
H. F. MAHLEIN,‡ T. VON EGIDY, AND W. KAISER
Physics Department of the Technical University, Munich, Germany
AND
H. R. KOCH, U. GRUBER, B. P. K. MAIER, AND O. W. B. SCHULT
Physics Department of the Technical University, Munich, Germany and Research Establishment of the Danish Atomic Energy Commission, Risø, Roskilde, Denmark
AND
D. W. HAFEMEISTER§ AND E. B. SHERA
University of California, Los Alamos Scientific Laboratory, Los Alamos, New Mexico
(Received 5 August 1968)

Nuclear levels in Re^{186} have been investigated by combining the following experimental techniques: the study of (d, p) and (d, t) reactions with 12-MeV deuterons and a broad-range magnetic spectrograph; the investigation of γ transitions between 3.6 and 6.2 MeV from neutron capture using a Ge(Li) spectrometer; the measurement of (n, γ) radiation between 28 and 770 keV with a bent-crystal spectrometer; and the measurement of the (n, e^-) spectrum in the energy range 0–350 keV with a magnetic β spectrometer. With the aid of (d, p) angular distributions and transition multipolarities, the energy levels up to an excitation energy of approximately 500 keV have been interpreted as arising from the coupling of the proton orbital [402 ↑] to the neutron orbitals [512 ↓], [510 ↑], and [503 ↑]. A possible proton excited state at 314 keV has been classified as resulting from the configuration p[514 ↑]; n[512 ↓]. Many higher-lying levels have also been observed. A Coriolis band-mixing calculation has been performed in an attempt to understand further the Re^{186} level structure below 500 keV. The (d, p) intensity pattern of the ground-state rotational band is in considerable disagreement with theoretical prediction, and it is suggested that residual interaction effects may be severely distorting the simple two-particle wave functions of the low-lying configurations.

I. INTRODUCTION

THE odd-odd nucleus Re^{186} presents an interesting spectroscopic problem. Although this nucleus is characterized by a moderately strong deformation[1] $\beta \simeq 0.22$, it occupies a mass region where the deformation is beginning to change relatively rapidly as a

† Work supported by the U.S. and Danish Atomic Energy Commissions.
* Work taken in part from a thesis submitted by R. G. Lanier to the Florida State University in partial fulfillment for the requirements of a Ph.D. degree. Present address: Oak Ridge National Laboratory, Oak Ridge, Tenn.
‡ Work taken in part from a thesis submitted by H. F. Mahlein to the Fakultat für Allgemeine Wissenschaften der Technischen Hochschule, Munich, Germany. Present address: Central Laboratory of the Siemens AG, Munich Germany.
§ Present address: Carnegie Institute of Technology, Pittsburgh, Pa.
[1] L. Armstrong and R. Marrus, Phys. Rev. **138**, B310 (1965).

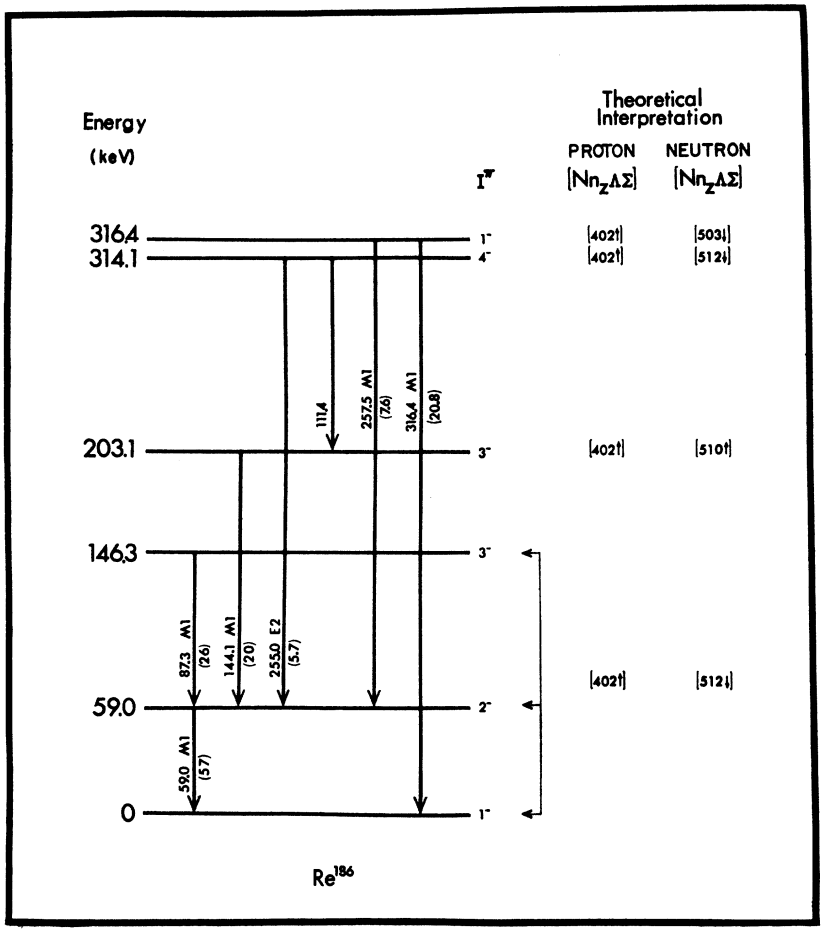

FIG. 1. Re^{186} level scheme as proposed by Prokofiev and Simonova (Ref. 10).

function of mass number. Thus, it is of interest to determine the extent to which the simple approach of coupling the Nilsson[2] orbitals of the 75th proton and 111th neutron can account for the observed level scheme.

From a consideration of the ground-state spins of the two neighboring isotopes and isotones of Re^{186}, the 75th proton should be characterized by the $[402\uparrow]^{3,4}$ configuration, while the 111th neutron is most probably in the $[512\downarrow]^{3,4}$ orbit. The Gallagher-Moszkowski[5] rule suggests that parallel coupling of the spins will be energetically favored; consequently, $I^\pi = 1^-$ should be the ground state.

Atomic beam measurements by Doyle and Marrus[6] have established $I=1$ for the Re^{186} ground state. The negative parity of the state seems highly probable because of the relatively large logft values associated with the β decay to the ground-state band of Os^{186}. Bogdan[7] has calculated logft values, spectral shapes, and β-γ correlation for this decay and found very good agreement with the experimental measurements by assuming that the Re^{186} ground-state configuration is $p[402\uparrow]$; $n[512\downarrow]$.

Other near-lying neutron orbitals which are expected at low excitation energies are $[510\uparrow]$, $[503\uparrow]$, $[505\downarrow]$, and $[651\downarrow]$. When coupled to the proton orbital $[402\uparrow]$, these configurations are expected to give rise to rotational bands having $K^\pi = (2^-, 3^-)$, $(1^-, 6^-)$, $(2^-, 7^-)$, and $(2^+, 3^+)$, respectively. In Re^{187}, a level at 206.24 keV is observed to have a lifetime of 5.6×10^{-7} sec and, because of its decay properties, has been assigned the $[514\uparrow]$ configuration.[3] Coupling this proton orbital to the neutron configurations $[512\downarrow]$ and $[510\uparrow]$ suggests rotational bands having $K^\pi = (3^+, 6^+)$ and $(5^+, 4^+)$.

Previous studies of Re^{186} have primarily utilized information obtained from various decay processes fol-

[2] S. G. Nilsson, Kgl. Danske Videnskab. Selskab, Mat.-Fys. Medd. **29**, No. 16 (1955).

[3] *Nuclear Data Sheets*, compiled by K. Way *et al.* (Printing and Publishing Office, National Academy of Sciences–National Research Council, Washington, D.C. 20025), NRC B1-1-84.

[4] *Nuclear Data Sheets*, compiled by K. Way *et al.* (Printing and Publishing Office, National Academy of Sciences–National Research Council, Washington, D.C. 20025), NRC B1-2-24.

[5] C. J. Gallagher and S. A. Moszkowski, Phys. Rev. **111**, 1282 (1958).

[6] W. M. Doyle and R. Marrus, Nucl. Phys. **49**, 449 (1963).

[7] D. Bogdan, Nucl. Phys. **48**, 273 (1963).

lowing thermal neutron capture by Re^{185}. Using a crystal spectrometer, Schult *et al.*[8] have accurately measured the energies of 11 transitions in Re^{186}. Based on internal conversion measurements with a magnetic β spectrometer, Prokofiev and Simonova[9,10] have assigned multipolarities to six of these transitions. Berestovoy, Kondurov, and Loginov[11] have applied the γ-γ coincidence method using scintillation counters to investigate the low-energy γ radiation from Re^{186}. These authors observed the 62±3-, 100±4-, 142±3-, 210±4-, and 255±6-keV transitions in the delayed coincidence spectrum with a lifetime of $(11.8\pm1.20)\times10^{-9}$ sec. The results of these earlier investigations are summarized in Fig. 1 in the decay scheme proposed by Prokofiev and Simonova.[10]

In this paper we present a more detailed experimental investigation of the level scheme of Re^{186} conducted in four different laboratories: at the Florida State University, utilizing the $Re^{185}(d, p)$ Re^{186} and $Re^{187}(d, t)$ Re^{186} reactions; at Risø, Denmark, and the Los Alamos Scientific Laboratory, where low-energy and both low- and high-energy γ rays, respectively, have been measured from the reaction $Re^{185}(n, \gamma)$ Re^{186}; and at Munich, Germany, through the study of the conversion electron spectrum following thermal neutron capture by Re^{155}. Part of these results have been briefly discussed elsewhere.[12,13]

II. EXPERIMENTAL METHODS AND RESULTS

The (d, p), (d, t), and high-energy (n, γ) results provide a convenient starting point for the construction of the nuclear level scheme because they directly yield a considerable fraction of the excited states. These experimental methods will be discussed first. High-resolution, low-energy (n, γ) results very accurately determine level energies and assist in the discovery of additional levels through a judicious use of energy combinations. These measurements are discussed next. Finally, the results of the (n, e^-) experiments are discussed. These data in combination with the results of low-energy (n, γ) studies permit the determination of transition multipolarities, mixing ratios, and total intensities. Consequently, the parity of a level can generally be determined and limits can be put on its spin.

A. (d, p) and (d, t) Studies

These reactions were studied using the Florida State University tandem Van de Graaff accelerator[14] and a Browne-Buechner[15] broad-range magnetic spectrograph. Deuterons with an energy of 12 MeV were focused on a target containing the separated isotope of Re^{185} (Re^{187}). The emerging protons (tritons) were momentum-analyzed by the magnet and detected by a set of three nuclear emulsion plates lying along the focal plane. In the (d, p) exposures, absorber foils were inserted in front of the plates to eliminate all but the proton tracks. Following a standard developing procedure, the plates were scanned for particle tracks per $\frac{1}{2}\times8$-mm strips.[16] The data presented are given as the number of proton (triton) tracks per $\frac{1}{2}$-mm strip as a function of the distance along the focal curve.[17]

The targets used in these experiments were composed of metallic rhenium and were prepared with the Florida State University isotope separator. Details of the target preparation have been published elsewhere.[18] A thin film of carbon—approximately 100–200 $\mu g/cm^2$—was employed as the target substrate. These targets possessed an enrichment of approximately 99% in the respective isotope; however, for the (d, p) reaction at forward angles, peaks due to various light impurities present in the substrate sometimes obscured the primary spectrum. In most cases, these impurities were identified through their large kinematic shift. An upper limit of 150 and 100 $\mu g/cm^2$ was determined for the Re^{185} and Re^{187} targets, respectively. These thicknesses were deduced directly from isotope-separator beam currents assuming 100% collection of this current as target.

An independent determination of the Re^{185} target thickness was performed by measuring the intensity of 12-MeV deuterons elastically scattered by the target prior to each long (d, p) exposure. At this energy, particularly at backward angles, the elastic cross section deviates considerably from the Rutherford prediction; consequently, a more realistic estimate of this cross section was obtained from scattering theory using

[8] O. W. B. Schult, B. Weckermann, T. v. Egidy, and E. Bieber, Z. Naturforsch. **18a**, 61 (1963).
[9] P. T. Prokofiev and L. I. Simonova, in Proceedings of the Sixteenth Annual All-Union Conference on Nuclear Spectroscopy and Structure of Atomic Nuclei, Moscow, 1966, p. 70 (unpublished).
[10] P. T. Prokofiev and L. I. Simonova, Yadern. Fiz. **5** 697 (1967) [English transl.: Soviet Phys.—Soviet J. Nucl. Phys. **5**, 493 (1967)].
[11] A. M. Berestovoy, I. A. Kondurov, and Yu. E. Loginov, Izv. Akad. Nauk SSSR, Ser. Fiz. **30**, 209 (1966).
[12] H. F. Mahlein, thesis submitted to the Fakultät für Allgemeine Wissenschaften der Technischen Hochschule, Munich, 1967 (unpublished).
[13] T. v. Egidy, H. F. Mahlein, W. Kaiser, B. C. Dutla, A. Jones, and A. A. Suarer, in Diskunionstagung über Neutronenphysik an Forschungsreaktoren, Jülich, 1967, p. 56 (unpublished).
[14] Supported by the U.S. Atomic Energy Commission and the Nuclear Program of the State of Florida and by the U.S. Office of Scientific Research under Contract No. AF OSR-62-423.
[15] C. P. Brown and W. W. Buechner, Rev. Sci. Instr. **27**, 899 (1956).
[16] We are very grateful to Miss Veronica Bryant, Mrs. Sue Hipps, Mrs. Mary Jones, and Mrs. Hazel Benton for their careful plate counting.
[17] For more details of the experimental procedure, refer to M. N. Vergnes and R. K. Sheline, Phys. Rev. **132**, 1736 (1963); R. A. Kenefick and R. K. Sheline, *ibid.* **133**, B11 (1964); W. N. Shelton and R. K. Sheline, *ibid.* **133**, B624 (1964).
[18] K. E. Chellis and R. K. Sheline, Nucl. Instr. Methods **54**, 139 (1967).

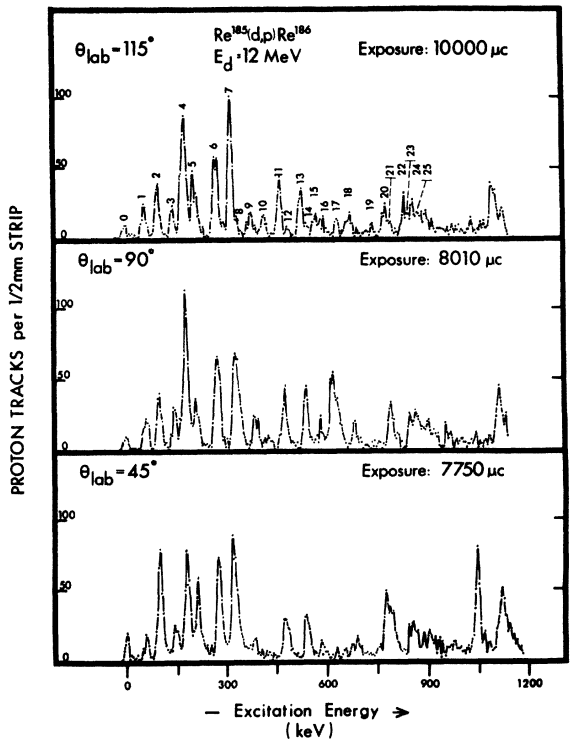

FIG. 2. Proton spectra from the reaction $Re^{185}(d, p)Re^{186}$ observed at different laboratory angles.

the optical-model parameters of Perey and Perey.[19,20] From these results the Re^{185} target was determined to have a thickness of 85 ± 20 $\mu g/cm^2$. It must be remarked that this value only represents an average over all runs. Because of constant retuning of focusing controls and the physical movement of the target between exposures, the actual thickness "seen" by the beam varies between exposures. Slight alterations in the beam optic controls could have changed the effective target thickness, since the beam image was somewhat wider than the target spot.

The raw spectrograph data were routinely analyzed using the computer code STRILDE[21] written for the Florida State University CDC 6400 computer. This program decomposes the observed spectrum into a sum of symmetrical Gaussian functions each having a characteristic centroid and area, and determines the Q values and cross sections corresponding to these parameters.

The (d, p) spectra were analyzed at seven angles: 22.5°, 26°, 35°, 45°, 65°, 90°, and 115°, and typical exposures ranged from 5000 to 11 000 μC. The results of three of these exposures are presented in Fig. 2.

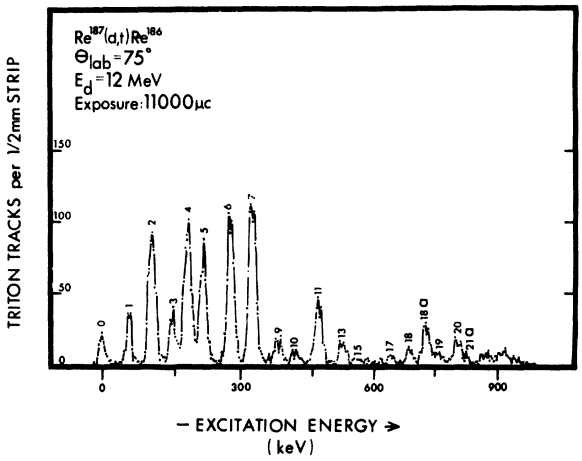

FIG. 3. Triton spectrum from the reaction $Re^{187}(d, t)Re^{186}$ observed at $\theta_{lab}=75°$. The numbering sequence of the (d, t) peaks is identical with that used for the (d, p) spectra in Fig. 2. The letter "a" following a number implies that the triton excited state is not populated in the (d, p) process.

TABLE I. Energy levels and relative cross sections for the reactions $Re^{185}(d,p)Re^{186}$ and $Re^{187}(d,t)Re^{186}$.

Level	(d,p) Energy[a] (keV)	(d,p) Rel. int.[c] (65°)	(d,t) Energy[b] (keV)	(d,t) Rel. int.[c] (75°)
0	0 (2)[d]	0.27	0 (2)[e]	0.17
1	60.6 (2)	0.40	58.0 (2)	0.27
2	101 (2)	1.00	100 (2)	1.00
3	147 (2)	0.50	145 (2)	0.36
4	180 (2)	2.10	177 (2)	1.10
5	210 (2)	1.17	211 (2)	0.80
6	273 (2)	2.03	272 (2)	1.10
7	320 (2)	2.09	321 (2)	1.29
8	(342)[f] (2)	0.26		
9	377 (2)	0.43	378 (2)	0.17
10	414 (3)	0.39	420 (4)	0.08
11	468 (2)	0.93	470 (2)	0.45
12	495 (3)	0.12		
13	533 (3)	1.11	535 (2)	0.15
14	547[g]	0.26		
15	567	0.30	(565)[f]	0.40
16	576	0.44		
17	643	0.10	647	0.05
18	683	0.49	687	0.10
18a[h]			726	0.30
19	747	0.38	755	0.10
20	795	0.63	797	0.20
21	803	0.40		
21a[h]			820	0.04
22	854	Complex		
23	867	Complex		
24	881	Complex		
25	900	Complex		

[a] Energies are the average values of seven independent experiments.
[b] Energy values are the results of only one exposure.
[c] Normalized to the level at approximately 100 keV.
[d] Quoted error is the standard deviation of the average.
[e] Estimated errors.
[f] Level is doubtful.
[g] Errors are not statistically determined from this excitation energy to higher excitations. Reasonable errors are 5–10 keV.
[h] Level is observed only in the (d, t) reaction.

[19] C. M. Perey and F. G. Perey, Phys. Rev. **132**, 755 (1963).
[20] We are indebted to Dr. W. J. Thompson for performing these calculations.
[21] We wish to thank H. Kaufmann for making a modified version of his program STRIP available to us.

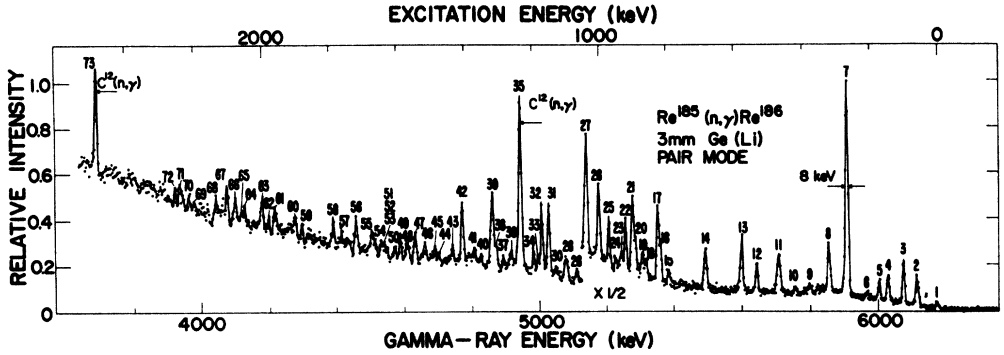

FIG. 4. High-energy γ-ray spectrum from the $Re^{185}(n,\gamma)Re^{186}$ reaction observed with the Los Alamos Ge(Li) spectrometer. The lines are numbered to correspond with Table II.

The experiments have determined the ground-state (d,p) Q value to be 3939 ± 25 keV. This compares with the result $Q=(6179.5\pm3.0)-(2224.5\pm0.1)=3955.0\pm3.0$ keV determined from the binding energy of the last neutron in Re^{186} as measured in the reaction $Re^{185}(n,\gamma)Re^{186}$ (Sec. II B).

One (d,t) exposure of 11 000 μC was taken at a scattering angle of 75°. The results of this experiment are given in Fig. 3. The ground-state Q value for the (d,t) reaction was found to be -1055 ± 25 keV. This compares favorably with the value -1063 ± 70 keV based on the mass table of Mattauch, Thiele, and Wapstra.[22] The excitation energies and relative cross sections for the levels observed in both the (d,p) and (d,t) experiments are listed in Table I.

B. High-Energy (n,γ) Spectrum

The high-energy neutron-capture γ-ray spectrum was measured with a lithium-drifted germanium spectrometer. A typical spectrum is shown in Fig. 4. Details of the spectrometer are given in Ref. 23. For the present measurements, a Ge detector with a 3-mm depletion depth was used. This detector, in combination with a field-effect transistor preamplifier, yields a linewidth [full width at half-maximum (FWHM)] of 8 keV at 8 MeV. The spectrometer calibration was performed using as standards the energies[24] and cross sections[25] of the nitrogen lines emitted from a melamine target.

The Re^{185} target used in these measurements was obtained from Oak Ridge National Laboratory[26] and consisted of 150 mg of rhenium metal, enriched to 96.6% in Re^{185}. The neutron-capture cross section of Re^{185} is 110 b and the cross section of Re^{187} is 71.3 b,[27] and hence the above enrichment results in 97.7% of the total capture in Re^{185}. The data from a separate study of an enriched Re^{187} target[28] have been used to correct the present data for the small contamination from this isotope, and all the lines identified in Fig. 4 can be attributed to the $Re^{185}(n,\gamma)Re^{186}$ reaction.

The measured γ-ray energies and intensities from the reaction $Re^{185}(n,\gamma)Re^{186}$ are listed in Table II. The ground-state spin-parity assignment of Re^{185} is $\frac{5}{2}^+$,[3] and the spin-parity assignment of the compound state formed after thermal neutron capture is therefore 2^+ or 3^+. Assuming, as is overwhelmingly the case, that only $E1$ and $M1$ transitions occur from the capture state to lower levels, transitions are permitted only to states with spins and parities $1^\pm$–$4^\pm$. The more energetic of the observed transitions, the energies of which differ from the binding energy by less than 2 MeV, are assumed to correspond to primary transitions from the capture state directly to a low-lying level.

The binding energy of the last neutron in Re^{186} has been determined to be 6179.5 ± 3.0 keV. This value was determined by combining the γ-ray energy of lines 2–4 with the excitation energies of the corresponding levels obtained from the low-energy capture γ-ray studies (columns 1 and 2 in Table III). The excitation energies of the remaining levels of Re^{186} calculated using the (n,γ) value for the binding energy are listed in Table II. A minimum error of ±3 keV has been assigned to all of the primary γ-ray energies, since these values include any possible uncertainty in the N^{15} neutron binding energy upon which the energy calibration is based. The excitation energies, which involve only energy differences, are assigned smaller errors.

---

[22] J. H. E. Mattauch, W. Thiele, and A. H. Wapstra, Nucl. Phys. **67**, 32 (1965).

[23] E. T. Jurney, H. T. Motz, and S. H. Vegors, Nucl. Phys. **A94**, 351 (1967).

[24] R. C. Greenwood, in *Proceedings of the Conference on Slow-Neutron Capture Gamma-Rays*, edited by H. H. Bolotin (Argonne National Laboratory, Argonne, Ill., 1966), Report No. ANL-7282 (1966).

[25] H. T. Motz, R. E. Carter, and W. D. Barfield, *Pile Neutron Research in Physics* (International Atomic Energy Agency, Vienna, 1962), p. 234.

[26] Union Carbide Corporation, Separated Isotopes Division, Oak Ridge, Tenn. 37831.

[27] *Neutron Cross Sections*, compiled by M. O. Goldberg *et al.* (Clearinghouse for Federal Scientific and Technical Information, National Bureau of Standards, U.S. Department of Commerce, Springfield, Va. 22151), BNL-325, 2nd ed., Suppl. 2, p. 75-185-1.

[28] E. B. Shera, H. R. Koch, U. Gruber, B. P. K. Maier, O. W. B. Schult, R. G. Lanier, and R. K. Sheline (to be published).

TABLE II. The γ-ray energies and the intensities (γ rays per 1000 neutrons captured by Re^{185}). The excitation energies have been derived using a neutron binding energy of 6179.5 keV.

Line No.	γ-ray energy (keV)	Excitation energy (keV)	Intensity γ/1000 neutrons captured by parent	Comments
1	6179.1±5.0	0 (0.4±2.0)	0.23±0.07	
2	6120.3±3.0	59.2±0.5	1.8±0.4	
3	6080.1±3.0	99.4±0.5	2.2±0.5	
4	6033.4±3.0	146.1±0.5	1.4±0.3	
5	6006.2±3.0	173.3±1.0	0.89±0.22	
6	5969.4±5.0	210.1±2.5	0.31±0.14	
7	5911.1±3.0	268.4±1.0	11.4±2.4	
8	5857.8±3.0	321.7±1.5	2.5±0.6	
9	5801.0±5.0	378.5±3.0	0.34±0.18	
10	5757.3±5.0	422.2±3.0	0.27±0.13	
11	5710.2±3.0	469.3±1.5	2.3±0.5	
12	5645.6±3.0	533.9±1.5	1.2±0.3	
13	5602.4±3.0	577.1±1.5	2.2±0.5	
14	5494.3±3.0	685.2±2.0	1.7±0.4	
15	5385.2±4.0	794.3±3.0	0.45±0.22	
16	5362.3±5.0	817.2±3.0	0.61±0.20	
17	5354.8±3.0	824.7±2.0	3.0±0.7	
18	5319.2±4.0	860.3±3.0	0.76±0.26	
19	5307.8±4.0	871.7±3.0	1.00±0.32	
20	5287.7±4.0	891.8±3.0	0.62±0.21	
21	5279.2±3.0	900.3±2.0	3.3±0.7	
22	5257.3±3.0	922.2±2.0	1.4±0.3	
23	5245.3±4.0	934.2±3.0	0.4±0.1	
24	5226.1±4.0	953.4±3.0	0.42±0.19	
25	5207.2±3.0	972.3±2.0	1.06±0.3	
26	5177.6±3.0	1001.9±2.0	2.6±0.6	
27	5140.2±3.0	1039.3±2.0	4.5±1.0	
28	5111.8±3.0	1067.7±2.0	0.55±0.11	
29	5080.7 ···	1098.8 ···	2.2±0.5	Complex
30	5048.9±5.0	1130.6±3.0	0.5±0.2	
31	5028.9±3.0	1150.6±2.0	4.8±1.1	
32	5008.3±3.0	1171.2±2.0	4.8±1.1	
33	4995.6±5.0	1183.9±3.0	0.71±0.32	
34	4982.6±4.0	1196.9±3.0	1.02±0.36	
35	4945.3±3.0	··· ···	··· ···	$C^{12}(n,\gamma)C^{13}$
36	4915.6±4.0	1263.9±3.0	1.00±0.36	
37	4891.8±4.0	1287.7±3.0	0.42±0.11	
38	4872.8±5.0	1306.7±3.0	1.3±0.4	
39	4861.1±3.0	1318.4±2.0	6.0±1.3	
40	4828.6±5.0	1350.9±3.0	0.50±0.23	
41	4809.0±5.0	1369.7±4.0	0.58±0.31	
42	4772.9±3.0	1406.6±2.0	3.7±0.7	
43	4743.0±3.0	1436.5±3.0	0.72±0.61	
44	4702.8±5.0	1476.7±4.0	0.82±0.24	
45	4690.9±5.0	1488.6±4.0	0.77±0.21	
46	4659.8±5.0	1519.7±5.0	1.6±0.6	
47	4632.4±3.0	1547.1±3.0	2.0±0.5	
48	4611.6 ···	1567.9 ···	1.6±0.4	Complex
49	4589.7±3.0	1589.8±3.0	1.4±0.3	
50	4572.1±4.0	1607.4±3.0	0.66±0.15	
51	4549.8±5.0	1629.7±4.0	0.28±0.7	
52	4542.2±5.0	1637.3±4.0	0.73±0.20	
53	4531.6±5.0	1647.9±4.0	1.16±0.29	
54	4514.4±5.0	1665.1±5.0	0.7±0.4	
55	4503.6±4.0	1675.9±4.0	1.2±0.3	
56	4455.6±3.0	1723.9±3.0	2.5±0.7	
57	4412.2±5.0	1767.3±4.0	0.81±0.45	
58	4388.1±4.0	1791.4±4.0	1.6±0.6	
59	4294.9±3.0	1884.6±4.0	0.91±0.23	
60	4274.4±4.0	1905.1±4.0	1.16±0.29	
61	4213.5±3.0	1966.0±4.0	1.7±0.5	
62	4194.5±3.0	1985.0±4.0	0.8±0.3	
63	4175.3±3.0	2004.2±3.0	1.8±0.4	
64	4124.0±4.0	2055.5±4.0	0.56±0.13	
65	4116.0±4.0	2063.5±4.0	0.43±0.10	
66	4096.7±3.0	2082.9±4.0	1.6±0.4	
67	4073.1±3.0	2106.4±4.0	2.2±0.6	
68	4038.3 ···	2141.2 ···	1.4±0.4	Complex
69	3974.9±4.0	2204.6±4.0	0.55±0.12	
70	3960.8±3.0	2218.7±4.0	0.74±0.17	
71	3934.0 ···	2245.5 ···	2.0±0.9	Complex
72	3918.4±3.0	2261.1±4.0	0.74±0.15	
73	3683.2±3.0	··· ···	··· ···	$C^{12}(n,\gamma)C^{13}$

C. Low-Energy (n, γ) Spectrum

1. *Risø Experiment*

The γ transitions from thermal neutron capture in a sample containing 79.2% Re^{185} and 20.8% Re^{187} have been measured with the bent-crystal spectrometer at Risø.[29] The energy region 28.5–1360 keV was automatically scanned, and except for very weak reflexes all measurements were manually made point by point. Strong lines were measured in the fifth-order reflection, medium-strong lines were studied in the third-order reflection, and weak lines were studied in the second-order reflection. A reflex width of 7 sec of arc was obtained corresponding to a resolution

$$\delta E/E \approx (1.4\times10^{-5})\,E\ (\text{keV})/n, \qquad (1)$$

where δE is the energy width of the reflexes (FWHM) and n is the order of reflection. A great number of γ-ray lines were observed. Most of these belong to transitions in Re^{186}, some are transitions in Re^{188}, and a few result from the radioactive decay of these isotopes. A second run with a rhenium target enriched in Re^{187} permitted the assignment of the observed γ-ray lines to the proper rhenium isotope. The Re^{188} data will be published separately.[28]

The results of the Re^{186} measurement are contained in columns 1–4 of Table III. The energies of the observed transitions (column 1) have been obtained using the x rays of rhenium as standards. The transition intensities (γ rays per 100 neutrons captured) were obtained through a comparison with the known decay to Os^{186} (column 3). This is a convenient standard because the γ rays resulting from this decay are observed simultaneously with the γ rays from neutron capture. The intensity errors (column 4) are generally 10–15% for stronger peaks. Because of the poorly defined γ self-absorption of the source, an additional intensity error of up to 50% must be taken into account when one compares transitions above 200 keV with transitions below 100 keV.

The observed x-ray lines are very strong and have large natural widths. As a result, their reflexes have broad and intense tails which reduce the sensitivity of the spectrometer. Consequently, weak γ rays having energies close to the K x-ray energies of rhenium, osmium, or tungsten may well escape detection. Another essential fact which must be emphasized concerns the energy dependence of the resolution [Eq. (1)] and the large number of γ rays emitted from a nucleus following neutron capture. Hence, in cases of multiplets, the energy and intensity given necessarily apply to the center of gravity of the complex groups.

2. *Los Alamos Experiment*

In addition, the γ-ray spectrum from the $Re^{185}(n, \gamma)$ reaction was measured over the energy range 50–1000 keV, using the Ge(Li) detector surrounded by the NaI annulus described in Sec. II B. The Re^{185} target and the geometrical arrangement were identical to that employed in the measurement of the high-energy γ spectrum. The annulus was operated in an anticoincidence mode to reduce the Compton background. In the energy range studied, 63 lines were observed. The energies (column 6, Table III) are in good agreement (within 1 keV or less) with the energies obtained from the bent-crystal spectrometer (Sec. II C 1). The γ-ray intensities (column 8) are relative values and are normalized with respect to the line at 214.6±1.0 keV.

In addition to the prompt spectrum, the transitions arising from the decay of both Re^{186} and Re^{188} have been observed. None of these decay transitions appear to conflict with the spectrum obtained from the Risø measurements.

D. Internal Conversion Studies

The conversion electron spectrum of Re^{186} has been measured with the β spectrometer installed at the Munich Research reactor.[30] The target used in these experiments was made from a sample of 96.66%-enriched Re^{185} metal powder obtained from the Oak Ridge National Laboratory.[26] Although the enriched sample contained an admixture of 3.34% Re^{187}, this did not greatly disturb the measurements. The rhenium target had an area of 12×80 mm^2 and a thickness of 0.4 mg/cm^2. The target substrate was aluminum, having a thickness of approximately 0.2 mg/cm^2.

In cooperation with Maier,[31] the following procedure was used to prepare a suitable target. A sample of 25 mg of enriched rhenium metal powder was dissolved in a hydrogen-peroxide solution in a quartz-glass tube. The resulting solution was dried in a vacuum and a red oxide was recovered. The metallic oxide was subsequently evaporated onto a rotating sheet of aluminum foil. The evaporation was performed by electric heating under high-vacuum conditions. Rotation of the aluminum foil ensured that the vaporized oxide would be uniformly collected and also prevented local heating of the foil which might have caused a reevaporation of the collected oxide. Because of the hygroscopic nature of the rhenium oxide, the target was immediately placed into an electric oven, where it was reduced in a hydrogen flux at approximately 400°C.

Conversion electrons were searched for in an energy range 0–720 keV. A total of 4000 experimental points was measured. In order to cover the energy range adequately, each point was measured for a period of

[29] U. Gruber, B. P. Maier, and O. W. B. Schult, Kerntechnik **5**, 17 (1963); B. P. Maier, U. Gruber, and O. W. B. Schult, *ibid.* **5**, 19 (1963); O. W. B. Schult, U. Gruber, and B. P. Maier, *ibid.* **7**, 101 (1965).

[30] T. von Egidy, Ann. Physik **9**, 221 (1962); W. Nörenberg, Z. Angew. Phys. **17**, 452 (1964); E. Bieber, Z. Physik **189**, 217 (1966); Th. W. Elze, *ibid.* **194**, 280 (1966).

[31] R. Maier, Diplomarbeit, Physik-Department TH München, 1966 (unpublished).

TABLE III. Low-energy γ-ray and electron data from $Re^{185}(n,\gamma)Re^{186}$. The symbols listed in column 5 are to be interpreted as follows: γ line is weak and its existence is questionable; d—the line is due to radioactive decay; +—the γ line is complex. In column 20, a a positive sign indicates that the electron intensity in column 13 has not been corrected for this superimposed electron line. The in- known relative intensities of the Auger lines [I. Bengström and C. Nordling, in *Alpha-, Beta-, and Gamma-Ray Spectroscopy*, edited by certainties are statistical errors only.

		Risø				Los Alamos				
1 E_γ (keV)	2 ΔE_γ (keV)	3 $I_\gamma/100n$	4 $\Delta I_\gamma/I_\gamma$ (%)	5 Comment	6 E_γ (rel.)	7 ΔE_γ (rel.)	8 Rel. int.	9 $\Delta I_\gamma/I_\gamma$ (%)	10 Shell	11 E_e (keV)
40.350	0.003	1.44	15	X					L_1	27.84
									L_2	28.38
									L_3	29.84
									M	37.45
									N	39.79
56.408	0.003	0.25	15						L_1	43.96
59.009	0.004	13.0	10	X	60.8	0.5	>1.0	...	L_1	46.53
									L_2	47.07
									L_3	48.47
									M	56.15
									N	58.44
									O	59.02
										48.97
										50.46
										53.63
61.928	0.004	1.2	10	X					L_1	49.40
									M	59.02
									L_1	50.92
									M	60.62
64.42	0.04	0.056	15	X						
74.568	0.003	1.5	10	X					L_1	62.05
									L_2	62.63
									L_3	64.3
									M	71.69
86.84	0.04	0.24	20						K	15.12
87.266	0.004	2.0	10	X	87.2	0.5	0.20	25	K	15.64
									L_1	74.78
									L_2	
									M	84.35
92.122	0.004	0.59	10	?	92.0	0.7	0.05	30	K	20.4
									L_1	79.61
99.362	0.004	0.51	15	X	99.3	0.8	0.07	25	K	27.84
									L_1	86.9
									L_2	87.33
									L_3	88.85
99.696	0.004	0.27	20	X						
100.59	0.04	0.06	30							
100.91	0.03	0.06	30							
102.62	0.02	0.06	30							
103.310	0.006	1.22	15	X	103.5	0.8	0.12	25	K	31.75
103.59	0.04	0.08	20							
106.550	0.004	0.64	10						K	34.91
					107.0	1.4	0.08	25	L_1	94.03
108.16	0.04	0.07	30							
108.336	0.005	0.20	20							
108.58	0.04	0.02	...	*						
109.51	0.04	0.05	20						K	37.45
									L_1	96.89
110.240	0.004	0.21	15							
					111.4	0.5	0.32	20		
111.337	0.008	1.37	10	X					K	39.79
									L_1	98.93
111.674	0.006	1.6	15	?					M	108.67
									N	111.15
111.814	0.004	0.87	15						K	40.14
									L_1	99.31
									M	108.67
									N	111.15
112.12	0.05	0.03	...	*						
118.196	0.004	0.25	15		118.2	1.0	0.04	30		
122.525	0.005	1.5	20	?	122.6	0.5	0.22	25		

X—the transition is included in the decay shceme (Fig. 6); ?—the placement of the γ line in the level scheme is questionable; *—the negative sign preceding a shell designation and energy means that the intensity of the superimposed electron line has been subtracted; tensities of the KL_1L_1, KL_1L_2, and KL_1L_3 Auger lines were calculated from the measured intensity of the KL_2L_3 Auger line and the K. Siegbahn (North-Holland Publishing Co., Amsterdam, 1965), Vol. 2, p. 1523ff]. In all cases, the quoted energy and intensity un-

			Munich					
12 ΔE_e (keV)	13 $I_e/100n$	14 $\Delta I_e/I_e$ (%)	15 α_{expt}	16 α_{E1}	17 α_{E2}	18 α_{M1}	19 Multipolarity	20 Comment
0.03	20	25	14	0.265	1.38	9.14	$M1+(1+1.6, 1-0.6)\%$ $E2$	$-K$ 99.362
0.02	4.0	35	2.9	0.179	96.4	0.904		
0.04	2.1	30	1.5	0.238	111	0.113		
0.02	5.3	30						$+K$ 109.51
0.03	1.0	70	0.7					$-K$ 111.337
0.05	0.66	25	2.6	0.127	0.354	3.38	$M1+(E2)$	
0.03	38.5	15	3.0	0.114	0.316	2.97	$M1+<0.8\%$ $E2$	$-KL_1L_1$ (2.6)
0.03	4.5	20	0.35	0.0558	15.5	0.295		$-KL_1L_2$ (4.2)
0.04	0.6	30	0.05	0.0674	15.9	0.0342		$-KL_1L_3$ (2.8)
0.01	12	10						$+K$ 127.352
0.02	4.2	10	0.32					
0.02	2.3	15						$+M$ 61.928
0.04	4.0	20						KL_2L_3
0.04	1.9	25						KL_3L_3
0.07	0.4	25						Re^{186}(?)
0.03	2.5	30	2.1	0.102	0.280	2.58	$M1$	Complex(?)
0.02	2.3	15	1.9					+0 59.009
0.03	3.6	20						Re^{188}
0.05	0.34	30						Re^{188}
0.02	1.4	10	0.93	0.0669	0.175	1.5	$M1+E2$	
0.07	0.26	30	0.17	0.0273	5.0	0.148		
0.3	0.20	35	0.13	0.0313	4.94	0.0167		
0.04	0.45	20	0.30					
0.05	3.6	35	15	0.447	1.08	6.48	$M1$	
0.03	9.7	35	4.9	0.442	1.07	6.39	$M1(+<4\%$ $E2)$	
0.02	1.8	10	0.90	0.0463	0.126	0.950		
	<0.20		<0.10	0.0187	2.27	0.0105		
0.03	0.35	10	0.17					
0.1	1.8	35	3.1	0.385	0.968	5.47	$M1$	
0.07	0.48	35	0.81	0.0408	0.113	0.813		
0.03	20.4	25		0.318	0.838	4.40	$E2$	$+L_1$ 40.350
0.1	0.16	60	0.31	0.0342	0.0976	0.654		
0.04	0.68	10	1.33	0.0112	1.35	0.0637		
0.02	0.51	15	1.00	0.0122	1.20	0.00712		
0.09	1.5	40		0.288	0.777	3.94		Complex
0.03	1.4	70	2.2	0.266	0.732	3.60	$M1+E2$	
0.04	0.13	50	0.20	0.0289	0.0842	0.535		
0.02	5.3	30		0.248	0.694	3.33	$(M2, E2+E0)$	$+M$ 40.350
0.04	0.22	30	4.4	0.0271	0.0793	0.495		
0.03	3.3	45	2.4	0.238	0.672	3.17	$M1+(E2)$	$-N$ 40.350
0.30	0.81	10	0.59	0.0260	0.0764	0.472		
0.06	0.15	25						$+M$ 111.674
0.07	0.23	20						$+M$ 111.814
								$+L_1$ 123.507
								$+N$ 111.674
								$+N$ 111.814
0.04	3.8	20		0.236	0.667	3.14		Complex
0.05	0.57	25		0.0257	0.0758	0.467		Complex
0.06	0.15	25						$+M$ 111.337
0.07	0.23	20						$+L_1$ 123.507
								$+N$ 111.337

TABLE III

	Risø				Los Alamos					
1 E_γ (keV)	2 ΔE_γ (keV)	3 $I_\gamma/100n$	4 $\Delta I_\gamma/I_\gamma$ (%)	5 Comment	6 E_γ (rel.)	7 ΔE_γ (rel.)	8 Rel. int.	9 $\Delta I_\gamma/I_\gamma$ (%)	10 Shell	11 E_e (keV)
122.63[a]	0.03	0.5	50	d					K	53.2
									L_2	110.97
									L_3	112.31
									M	120.3
										110.09
										119.64
123.507	0.006	0.38	15						K	51.86
									L_1	111.15
125.35	0.05	0.04	30							
127.352	0.004	0.69	15	X	127.3	0.7	0.07	25	K	56.15
									L_1	114.9
128.66	0.03	0.18	40							
134.158	0.016	0.13	15							
135.25	0.08	0.04	...	*						
135.74	0.04	0.04	20							
137.150	0.004	9.9	10	d					K	63.27
									L_2	124.71
									L_3	126.24
									M	134.51
									N	136.68
138.22	0.04	0.07	20							
139.416	0.007	0.32	10		139.1	1.5	0.15	45	K	67.88
140.095	0.005	0.64	15						K	68.43
									L_1	127.60
140.924	0.010	0.09	15							
141.257	0.005	0.45	10						K	69.59
									$L_{1,2}$	129.1
142.80	0.04	0.14	20							
143.919	0.005	1.3	10						K	72.18
					144.1	0.8	0.65	25	L_1	131.27
144.152	0.005	4.3	10						K	72.49
									L_1	131.27
144.37	0.06	0.08	30							
145.131	0.008	0.11	20							
146.273	0.012	0.17	15	X						
147.417	0.006	1.4	10	?					K	75.66
					147.8	0.8	0.25	25	L_1	134.51
148.09	0.06	0.04	20	?						
148.37	0.06	0.09	20	X						
148.994	0.005	0.68	20	?					K	77.21
149.520	0.005	0.81	15						K	77.76
150.500	0.005	0.57	15						K	
					151.0	0.9	0.41	25		
151.686	0.005	2.8	10	X					K	79.98
									L_1	138.98
									M	148.5
157.02	0.03	0.09	20							
158.68	0.04	0.07	20							
158.93	0.04	0.04	40							
160.07	0.06	0.14	20							
161.68	0.06	0.05	20							
163.31	0.06	0.11	30							
164.466	0.008	0.38	15		163.4	1.3	0.06	35	K	92.93
166.494	0.08	0.04	20							
167.737	0.008	0.48	15	X	167.8	1.1	0.09	30	K	
169.431	0.008	0.30	15	?					K	97.7
170.47	0.08	0.07	25	+						
171.15	0.08	0.05	25	+						
172.28	0.08	0.04	20							
174.271	0.009	1.0	15	X					K	102.61
					175.3	0.8	0.26	25	L_1	161.58
176.112	0.008	0.42	15	X						
									K	104.67
176.552	0.008	0.34	15						L_1	163.72
177.244	0.008	0.22	15	+					K	105.72
179.448	0.007	0.27	15	?	180.5	2.5	0.04	35		
182.189	0.008	0.29	15	+					K	110.7

(*Continued*)

			Munich					
12 ΔE_e (keV)	13 $I_e/100n$	14 $\Delta I_e/I_e$ (%)	15 α_{expt}	16 α_{E1}	17 α_{E2}	18 α_{M1}	19 Multipolarity	20 Comment
0.1	0.32	25	0.64		0.572		$E2$	W^{186}
0.09	0.267	10	0.53		0.470			
0.07	0.222	5	0.44		0.395			
0.2	0.10	15	0.2					
0.04	0.48	20						Re^{186}(?)
0.05	0.17	25						Re^{186}(?)
0.08	0.80	30	2.1	0.183	0.551	2.36	$M1$	
0.07	0.23	20		0.0202	0.0609	0.352		$+N$ 111.337 $+N$ 111.674 $+N$ 111.814
0.01	1.2	10		0.169	0.519	2.16	$M1+E2$	$+M$ 59.009
0.1	0.085	50	0.12	0.0188	0.0569	0.322		
0.02	3.4	15	0.34		0.425		$E2$	Os^{186}
0.02	2.98	5	0.30		0.340			
0.02	2.44	5	0.25		0.266			
0.03	1.48	5						$+L_1$ 147.417
0.04	0.48	5	0.050					
0.09	0.23	35	0.72	0.134	0.419	1.67	$E2+M1$	
0.04	0.32	20	0.50	0.132	0.415	1.65	$M1+E2$	
0.06	0.13	40	0.20	0.0149	0.0462	0.246		
0.09	0.48	35	1.1	0.130	0.407	1.61	$M1$	
0.1	0.094	35	0.21	0.0183	0.317	0.263		
0.05	0.94	25	0.72	0.124	0.389	1.53	$M1+E2$	
0.06	0.13	50	0.10	0.0140	0.0435	0.227		$-L_1$ 144.152
0.07	0.49	40	0.11	0.123	0.388	1.52	$E1$	
0.06	0.06	70	0.014	0.0139	0.0434	0.226		$-L_1$ 143.919
0.02	1.3	10	0.93	0.116	0.367	1.43	$M1+E2$	
0.03	1.48	5		0.0132	0.0413	0.212		$+M$ 137.150
0.04	0.55	20	0.81	0.113	0.358	1.39	$M1+E2$	
0.04	0.49	20	0.61	0.112	0.355	1.37	$M1+E2$	
	<0.12		<0.21	0.110	0.350	1.35	$E1$	
0.02	2.1	15	0.75	0.108	0.343	1.32	$M1+E2$	$+L_2$ 92.122
0.02	1.7	10		0.0123	0.0388	0.196		$+K$ 210.685
0.1	0.14	20						$+K$ 219.78 $+K$ 220.51
0.06	0.23	25	0.61	0.0881	0.280	1.05	$M1+E2$	
	<0.13		<0.27	0.0839	0.267	0.996	$E1, E2$	
0.1	0.11	35	0.37	0.0818	0.260	0.968	$E2$	
0.03	0.53	20	0.53	0.0763	0.242	0.895	$M1$	
0.08	0.16	15	0.16	0.00884	0.0278	0.132		
0.06	0.40	10		0.0743	0.236	0.869		Complex
0.11	0.12	30		0.00862	0.0271	0.128		Complex
0.09	0.25	20	1.1	0.0731	0.232	0.854	$M1$	
0.1	0.22	25	0.76	0.0682	0.216	0.791	$M1$	

TABLE III

Risø					Los Alamos					
1 E_γ (keV)	2 ΔE_γ (keV)	3 $I_\gamma/100n$	4 $\Delta I_\gamma/I_\gamma$ (%)	5 Comment	6 E_γ (rel.)	7 ΔE_γ (rel.)	8 Rel. int.	9 $\Delta I_\gamma/I_\gamma$ (%)	10 Shell	11 E_s (keV)
183.09	0.08	0.03	40	+						
186.00	0.08	0.06	20	+						
186.70	0.08	0.04	20							
187.77	0.10	0.03	...	*						
189.313	0.017	0.78	10		189.2	0.6	0.12	30	K	117.68
									$L_{1,2}$	177.0
190.73	0.08	0.07	20							
192.60	0.10	0.04	...	*						
193.95	0.10	0.09	20							
195.83	0.10	0.03	...	*						
196.98	0.10	0.03	...	*						
				(?)						
197.67	0.03	0.11	15							
					198.8	0.9	0.04	35		
200.981	0.016	0.23	15	?						
201.78	0.10	0.04	20	?	201.1	0.9	0.03	35		
202.64	0.02	0.12	15							
204.96	0.15	0.06	20							
209.82	0.02	0.32	15	?						
210.685	0.017	3.3	10	X	210.5	0.7	0.52	25	K	138.98
									L_1	198.13
									M	207.5
213.92	0.15	0.06	20	+						
214.648	0.008	6.5	10	X	214.6	0.6	1.00	20	K	143.01
									L_1	202.0
215.28	0.15	0.11	20							
217.91	0.10	0.09	20						K	146.5
218.69	0.10	0.06	20							
219.78	0.10	0.19	15	+						
									K	148.5
220.51	0.15	0.04	25							
221.76	0.10	0.07	15							
223.035	0.015	0.55	10	X	222.6	0.8	0.11	35	K	151.37
228.42	0.10	0.11	20							
230.65	0.15	0.04	25							
232.100	0.016	0.57	10	+	232.0	0.7	0.09	25	K	160.16
				(X)					$L_{1,2}$	219.68
237.60	0.15	0.09	20		236.5	1.7	0.02	35		
241.90	0.20	0.04	...	*						
246.81	0.20	0.10	20	+						
248.75	0.10	0.04	20							
249.65	0.10	0.05	20							
251.841	0.015	4.6	10		252.1	0.7	0.84	20	K	179.8
254.995	0.015	3.5	10	X					K	183.4
					256.4	0.8	0.82	20		
257.446	0.015	3.6	10	X					K	185.70
									L_1	244.70
259.40	0.10	0.11	15							
260.87	0.15	0.30	...						K	189.43
									L_1	248.1
261.266	0.012	1.7	10		260.8	0.8	0.36	25	K	189.43
									L_1	248.1
263.33	0.20	0.25	20	+						
				(X)						
266.02	0.20	0.15	20	+						
266.70	0.20	0.14	20	+						
269.79	0.20	0.04	...	*						
271.47	0.10	0.27	15	?	271.4	1.0	0.02	35		
278.82	0.10	0.12	15							
285.10	0.03	0.56	10		285.2	0.7	0.09	30	K	
286.45	0.15	0.22	15							
289.06	0.15	0.07	20							
295.88	0.15	0.17	20	+					K	223.8
				(?)						
301.36	0.15	0.14	20	+						
307.56	0.06	0.78	10		307.7	0.7	0.14	35	K	235.93
									$L_{1,2}$	295.7
316.473	0.020	6.4	10	X	316.5	0.6	0.96	25	K	244.70
									L_1	303.99
319.44	0.10	0.43	15	X						
					321.3	0.8	0.12	35		

(*Continued*)

			Munich					
12 ΔE_γ (keV)	13 $I_\gamma/100n$	14 $\Delta I_\gamma/I_\gamma$ (%)	15 α_{expt}	16 α_{E1}	17 α_{E2}	18 α_{M1}	19 Multipolarity	20 Comment
0.03	0.37	15	0.47	0.0620	0.195	0.711	$M1$	
0.2	0.089	35	0.11	0.00875	0.0969	0.114		
0.02	1.6	10		0.0474	0.147	0.527	$M1$	$+L_1$ 151.686
0.08	0.28	15	0.085	0.00563	0.0176	0.077		
0.1	0.076	20	0.023					
0.06	0.23	25	0.036	0.0452	0.140	0.501	$E1$	
0.3	0.056	25	0.0086	0.00538	0.0168	0.0735		
0.2	0.064	40	0.70	0.0435	0.135	0.480	$M1$	
0.1	0.14	20		0.0423	0.130	0.464		$+M$ 151.686
0.05	0.16	10	0.29	0.0411	0.127	0.450	$M1+E2$	
0.08	0.20	15	0.35	0.0372	0.114	0.403	$M1$	
0.09	0.11	30	0.19	0.00527	0.0449	0.0650		
0.1	0.14	20	0.030	0.0303	0.0918	0.321	$E1$	
0.2	0.076	35	0.022	0.0293	0.0888	0.310	$E1$	
0.03	0.89	5	0.25	0.0287	0.0867	0.302	$M1$	
0.04	1.1	10		0.00350	0.0108	0.0449		$+K$ 316.473
0.06	0.1	70	0.33	0.0278	0.0838	0.291		$+K$ 261.266
0.1	0.13	15		0.00339	0.0105	0.0433		$+L_1$ 261.266
0.06	0.48	15		0.0277	0.0835	0.290	$M1$	$+K$ 260.87
0.1	0.13	15		0.00338	0.0104	0.0431		$+L_1$ 260.87
	<0.04		<0.07	0.0225	0.0667	0.229	$E1$, ($E2$)	
0.2	0.063	20	0.37	0.0206	0.0606	0.207	$M1$	
0.08	0.14	10	0.18	0.0188	0.0548	0.187	$M1$	
0.3	0.038	35	0.049	0.00266	0.0165	0.0302		
0.04	1.1	5		0.0175	0.0510	0.173	$M1$	$+L_1$ 257.446
0.09	0.17	15	0.027	0.00217	0.00654	0.0256		

TABLE III

Risø					Los Alamos					
1 E_γ (keV)	2 ΔE_γ (keV)	3 $I_\gamma/100n$	4 $\Delta I_\gamma/I_\gamma$ (%)	5 Comment	6 E_γ (rel.)	7 ΔE_γ (rel.)	8 Rel. int.	9 $\Delta I_\gamma/I_\gamma$ (%)	10 Shell	11 E_s (keV)
321.70	0.20	0.21	20	*						
328.42	0.20	0.07	...	* (?)						
335.66	0.20	0.11	25							
341.38	0.15	0.26	15							
354.10	0.05	0.96	10						*K*	
					355.4	0.8	0.17	25		
355.63	0.05	0.27	15							
357.65	0.15	0.22	20							
360.43	0.04	0.97	15		361.0	0.9	0.17	25	*K*	288.7
									L_1	346.6
363.45	0.15	0.38	20							
					365.1	1.2	0.04	40		
366.84	0.15	0.22	20							
373.49	0.15	0.10	25							
378.42	0.05	1.65	10	X	378.7	0.7	0.23	25	*K*	306.65
380.72	0.20	0.2	40							
386.31	0.15	0.09	30	+						
390.91	0.05	3.3	10		390.9	0.6	0.52	20	*K*	
396.54	0.20	0.20	20							
401.3	0.3	0.10	40	+						
406.92	0.20	0.24	20		406.6	1.2	0.02	35		
411.18	0.20	0.32	20	?						
					412.4	1.0	0.11	30		
413.21	0.06	0.40	20							
418.37	0.20	0.26	20		418.4	1.2	0.09	35		
419.97	0.20	0.23	25							
426.42	0.20	0.17	25		425.8	1.2	0.02	35		
430.9	0.3	0.15	30							
434.16	0.20	0.23	25							
439.01	0.20	0.23	25							
469.39	0.20	0.22	25		470.6	1.5	0.03	35		
					475.7	1.5	0.12	35		
477.9	0.3	0.5	40	+						
479.3	0.3	0.7	40	+	479.8	0.8	0.18	30		
487.18	0.20	0.23	25							
496.59	0.20	0.47	20		496.7	0.6	0.09	35		
					504.8	0.8	0.07	35		
					518.0	0.8	0.06	35		
					524.4	1.5	0.02	50		
533.9	0.5	0.21	20		533.6	0.7	0.04	35		
550.9	0.5	0.22	20		550.7	1.1	0.07	35		
					556.3	1.0	0.04	35		
561.6	0.5	0.14	30							
580.4	0.5	0.18	25		580.2	1.1	0.05	35		
584.3	0.7	0.18	25		584.4	1.1	0.06	35		
					593.4	1.1	0.03	40		
					597.6	1.0	0.05	35		
607.5	0.8	0.31	30		607.1	1.0	0.09	35		
616.4	0.8	0.15	30		616.4	1.0	0.05	35		
621.0	0.8	0.14	30		621.5	1.0	0.07	35		
625.7	0.8	0.18	30	+	626.2	1.0	0.07	35		
631.0	0.8	0.36	30	+	630.9	0.7	0.11	35		
645.3	0.8	0.14	30		645.1	1.0	0.04	40		
651.3	0.8	0.11	30		651.6	1.0	0.05	40		
680.0	1.0	0.27	30		680.9	0.8	0.12	30		
689.9	1.0	0.19	30		689.9	1.0	0.10	30		
694.1	1.0	0.45	30		694.6	1.0	0.15	30		
715.1	1.0	0.27	30		714.3	1.7	0.15	30		
728.1	1.2	0.29	30		729.0	1.6	0.15	60		
					733.3	1.8	0.11	60		
					754.9	1.4	0.18	40		
761.6	1.0	0.39	30		761.7	1.4	0.14	50		
					766.3	1.4	0.13	60		
					772.8	2.0	0.10	70		
					781.2	2.0	0.06	70		
					796.5	1.5	0.03	70		
					815.3	1.5	0.05	70		
					835.5	1.3	0.10	50		
					843.7	1.4	0.09	50		

(*Continued*)

			Munich					
12 ΔE_e (keV)	13 $I_e/100n$	14 $\Delta I_e/I_e$ (%)	15 α_{expt}	16 α_{E1}	17 α_{E2}	18 α_{M1}	19 Multipolarity	20 Comment
	<0.04		<0.04	0.0134	0.0382	0.127	*E*1, *E*2	
0.1 0.3	0.12 0.059	15 70	0.124 0.06	0.0129 0.00161	0.0365 0.00478	0.122 0.0180	*M*1	
0.09	0.17	15	0.103	0.0116	0.0325	0.107	*M*1	
	<0.06		<0.02	0.0108	0.0301	0.0980	*E*1	

[a] The conversion electron lines of this transition have been measured only after reactor shut down.

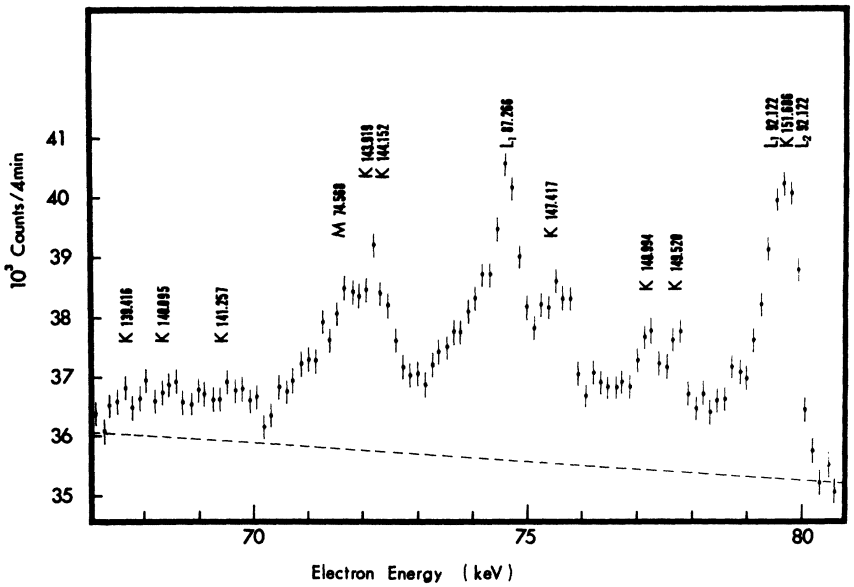

FIG. 5. A representative portion of the conversion electron spectrum of Re^{186} measured with the β spectrometer at Munich.

1 min. The range 0–400 keV was measured a second and a third time with a counting period of 4 min per point. In Fig. 5, a portion of the conversion electron spectrum measured with a counting period of 4 min per point is shown. A small range from 50 to 140 keV was also measured with a counting period of 10 min per point. In order to measure the low-energy conversion electrons from 0 to 60 keV, the target was negatively biased at 12 kV.[32] The entrance slit of the counter had an area of 2×15 mm^2 and the linewidth (FWHM) was about 0.3% at 150 keV.

Computer least-squares fitting was applied to the experimental data.[33] The energy calibration is based on the following γ lines obtained with the Risø bent-crystal spectrometer: 40.350 ± 0.003, 61.928 ± 0.004, 74.568 ± 0.003, 106.550 ± 0.004, 137.150 ± 0.004, 147.417 ± 0.006, 174.271 ± 0.009, 214.648 ± 0.008, 257.446 ± 0.015, 307.56 ± 0.06, and 316.473 ± 0.020 keV (Sec. II C 1).

The intensity calibration was performed with the decay lines 137.150 keV from Os^{186} and 122.63 keV from W^{186}. Both transitions have $E2$ character. Only the L_2 and L_3 lines of these transitions were used, because the intensity of the K line was affected to a poorly known extent by the absorption in the counter window. In the literature only the absolute intensities of the K lines are given.[34] Using the theoretical conversion coefficients of Sliv and Band,[35] we have obtained the absolute conversion electron intensities of the L_2 and L_3 lines. The result of the (n, e^-) studies are listed in columns 10–20 in Table III.

[32] T. von Egidy, E. Bieber, and Th. W. Elze, Z. Physik **195**, 485 (1966).

[33] Th. W. Elze, Z. Physik **194**, 280 (1966); T. von Egidy and Th. W. Elze, FRM Report No. 79, TH München, 1966 (unpublished).

[34] *Nuclear Data Sheets*, compiled by K. Way *et al.* (Printing and Publishing Office, National Academy of Sciences–National Research Council, Washington, D.C. 20025), NRC B1-2-11.

[35] L. A. Sliv and I. M. Band, in *Alpha-, Beta-, and Gamma-Ray Spectroscopy*, edited by K. Siegbahn (North-Holland Publishing Co., Amsterdam, 1965), Vol. 2, p. 1639ff.

III. DISCUSSION

A. Re^{186} Level Scheme

In this section we discuss in detail the construction of the level scheme given in Fig. 6. As far as has been possible, we have attempted to use only experimental data to arrive at the spin-parity assignments of the levels. The conversion electron data have permitted an unambiguous determination of the parity of almost all levels. However, for the unique determination of level spins, it was necessary to make reasonable assumptions about transition rates and to incorporate the predictions of a nuclear model. To this extent, the results summarized in the level scheme are not unambiguous.

1. 1^- *Ground State*

As previously pointed out (Sec. I), the Re^{186} ground state has $I=1$ and very probably negative parity. Arguments given in Sec. III A 2 imply that the ground state is populated in the (d, p) and (d, t) reaction, and through a primary γ transition originating from the compound system formed through slow neutron capture by Re^{185}. This compound system should have spin and parity 2^+ and/or 3^+ (Sec. II B). Therefore the 6179-keV transition is probably an $E1$ transition from the 2^+ component of the compound system to the 1^- ground state.

The spin-parity assignment of the ground state is consistent with either the 1^- component of the configuration $p[402\uparrow]$; $n[512\downarrow]$ or the 1^- component of $p[402\uparrow]$; $n[503\downarrow]$. Unfortunately, because of experi-

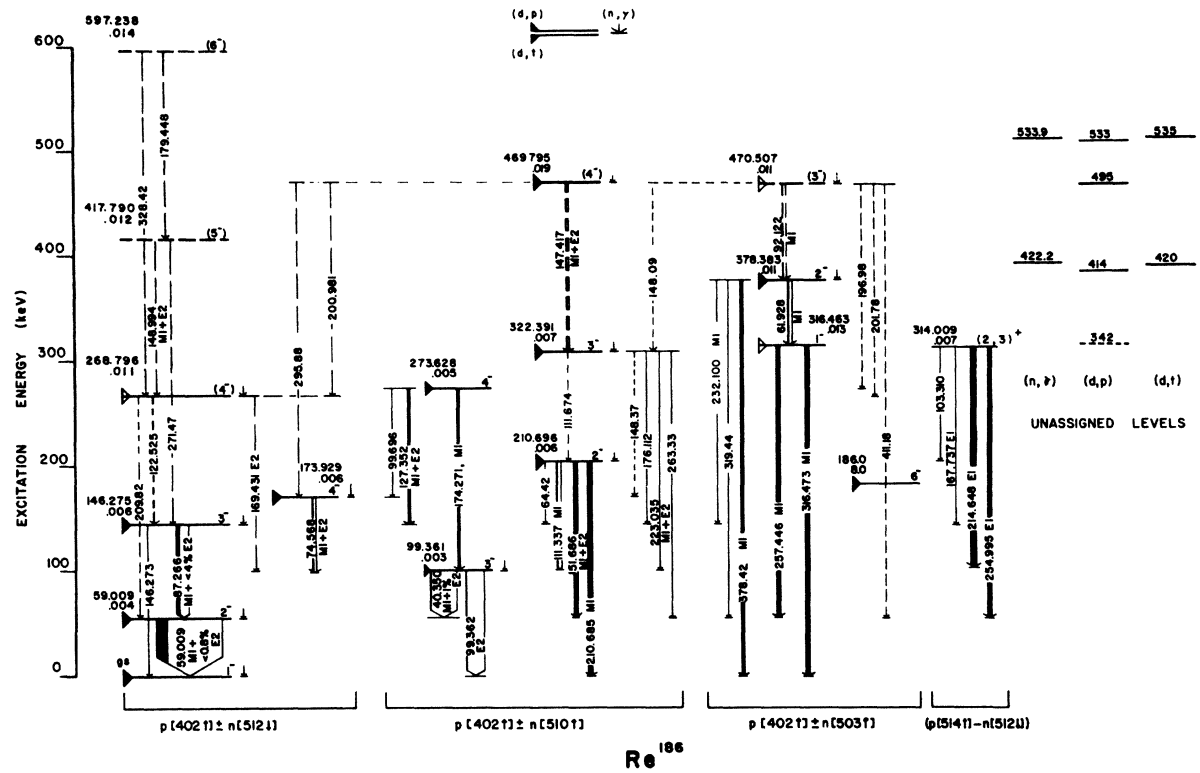

FIG. 6. Proposed level scheme of Re^{186}. Inasmuch as the experimental data are not sufficient to establish uniquely the identity of the levels observed, the spin-parity assignments given above are necessarily model-dependent. Parentheses indicate that the proposed assignment is based on incomplete or ambiguous information. The neutron-proton configuration given below each band shows the component of the wave function that is believed to predominate. A level represented by a dashed horizontal line implies that its existence is not firmly established by experiment. A triangle pointing down on the left-hand edge of a level signifies that the level is populated in the (d, t) reaction; a triangle pointing up to the left indicates population in the (d, p) experiments. Hollow triangles signify that the evidence for direct reaction population is not conclusive. High-energy (n, γ) population is indicated by a short vertical arrow. Transitions shown as dashed lines indicate that their placement in the level scheme is questionable.

mental uncertainties the observed proton angular distribution does not adequately distinguish these configurations. In addition to the previously mentioned results of Bogdan[7] (Sec. I), the former configuration is favored for two reasons. First, if $p[402\uparrow]$; $n[503\uparrow]$ were the ground-state configuration, it would imply a violation of the Gallagher-Moszkowski coupling rules which predict the 6^- level to be energetically favored. Second, the $[512\downarrow]$ neutron configuration in neighboring isotopes of Re^{186} is found to lie lower in energy than the $[503\uparrow]$ orbital. In W^{185} [3] the ground state is $\frac{3}{2}^-$ and a $K^\pi=\frac{7}{2}^-$ level is observed at 327 keV, while in Os^{187} [4] the $K^\pi=\frac{3}{2}^-$ state is seen at 10 keV and a level at 101 keV is tentatively assigned as $K^\pi=\frac{7}{2}^-$. It seems improbable, therefore, that the $[503\uparrow]$ orbital contributes to the 1^- ground state of Re^{186}. Consequently, in view of the experimental facts known about the Re^{186} ground state, together with the apparent systematics of the $[512\downarrow]$ and $[503\uparrow]$ orbitals in both W^{185} and Os^{187}, it appears most reasonable that the Re^{186} ground state is predominantly the $p[402\uparrow]$; $n[512\downarrow]$ configuration.

2. 2^- *Level at* 59 *keV*

The difference in energy between the two proton and triton groups with the highest energy observed in the (d, p) and (d, t) reactions is 60.6 ± 2.0 and 58.0 ± 2.0 keV, respectively. In addition, the energy difference between the two most energetic γ-ray transitions depopulating the Re^{186} compound nucleus is 58.8 ± 2.0 keV. The three energy differences observed from these independent measurements coincide within experimental error. It is concluded, therefore, that the same pair of levels is being populated by each process. The 59.009-keV transition observed in the low-energy (n, γ) studies and classified $M1$ through the (n, e^-) measurements was found to have the highest total intensity. Consequently this transition leads to the ground state, and this establishes a level at 59.009 keV. This excitation energy corresponds to the energy difference of the first two levels observed in the (d, p), (d, t), and high-energy (n, γ) experiments. This implies, therefore, that the ground state and 59-keV level are populated in these reactions.

The angular distribution of the proton groups associated with the population of the 59-keV level indicates $l=3$, 4, or 5, which does not allow the determination of the spin and parity of this state. The conversion electron data require negative parity and $I=0$, 1, or 2. The 0^- assignment would imply multipolarity $M2$ for the 6120-keV primary γ transition, and this is incompatible with the observed intensity of this line. The data considered to this point require a spin-parity assignment of 1^- or 2^- for the 59-keV state. In order to distinguish between these possibilities, however, it is necessary to have recourse to a nuclear model (Sec. III B).

If the 59-keV state has a spin-parity assignment of 1^-, we would most probably have to consider this level to be the band head of the $p[402\uparrow]$; $n[503\uparrow]$ configuration. In this case the Gallagher-Moszkowski coupling rules predict the 6^- component to have lower excitation energy. The (d, p) cross section of the 6^- band head is expected to be at least a factor of 2 or 3 larger than that of the ground state, and this level would be easily detected if it were situated between the ground and 59-keV levels. Furthermore, from the discussion in Sec. III A 1, we would expect the 1^- configuration at a higher excitation energy. For these reasons, the spin-parity assignment of 2^- is preferred for the 59-keV level.

A 2^- level at this excitation energy can be considered as either the second member of the ground-state rotational band or the band head of the $p[402\uparrow]$; $n[510\uparrow]$ configuration. The former interpretation yields a rotational parameter $\hbar^2/2\mathcal{I}=14.75$ keV, which seems reasonable when compared with those of Re^{185} and Re^{187} (17.6–19.2 keV) and of W^{185} and Os^{187} (12.0–13.0 keV).[3,4] In accordance with the Gallagher-Moszkowski coupling rules, the latter interpretation requires a 3^- band head to lie between the ground state and 59-keV level. No such level has been observed; consequently, the 2^- level appears to be most reasonably interpreted as the first member of the ground-state rotational band.

3. 3^- *Level at* 99 *keV*

A level at 99 keV is populated through the (d, p), (d, t), and high-energy (n, γ) reactions. The low-energy conversion electron data independently require this state because the total intensity of the 40.3-keV line is so large that this transition can only feed the 59-keV level. The assumption that the 40.3-keV transition feeds the ground state contradicts the requirement that the total ground-state population cannot exceed 100%. In addition, the 99-keV level is obtained through a well-satisfied energy combination with the 59.009-, 40.350-, and 99.362-keV transitions. The chance for this combination to occur by accident is very small and reduced by another factor of 2 because of the multipolarities of the 40.3- and 99.3-keV lines, which imply negative parity and spin 1, 2, or 3 for the 99-keV state.

Spin 1 or 2 can be understood only if the $M1$ component of the 99-keV ground-state transition is very strongly hindered in comparison with the $E2$ part. The very small $E2$ admixture in the 40.3-keV transition between the 99-keV level and the 2^- member of the ground-state rotational band implies that the $M1$ component should not be hindered if the spin possibilities of the 99-keV state and the spin of the ground state allow this type of radiation. Consequently, it is concluded that the 99-keV level has $I=3$. This result is consistent with the (d, p) angular distribution which is dominated by an $l=1$ component.

In view of the energy of the 99-keV state, it seems improbable that it is the 3^- rotational member of the ground band. The level appears most reasonably interpreted as the $K^\pi=3^-$ band head of the $p[402\uparrow]$; $n[510\uparrow]$ configuration. The strong (d, t) cross section for the excitation of this level implies that the intrinsic neutron wave function has appreciable hole character. This observation is consistent with the systematics of the $[510\uparrow]$ orbital in neighboring isotones of Re^{186}.[3,4] On the basis of our assumption for the structures of the 99-, 59-keV, and ground levels and the 1% admixture of $E2$ in the 40.3-keV transition as determined by internal conversion measurements, one can estimate the intensity of the 99.3-keV $E2$ transition according to Alaga's rule.[36] The result of this calculation is $0.9/100n \leq I_\gamma$ ($E2$, 99 keV) $\leq 5.7/100n$ and is somewhat larger than the experimental value $0.7/100n$, but the agreement still appears favorable in view of the large experimental uncertainties and the fact that mixing has been neglected.

4. 3^- *Level at* 146 *keV*

The (d, p), (d, t) and high-energy (n, γ) measurements reveal a level at 146 keV. The high-energy (n, γ) results require the level to be 86.9 ± 0.7 keV above the 59-keV state. The 87.266- and 146.273-keV transitions form a closed loop with the 59.009-keV level. The predominant $M1$ character of the 87.2-keV line implies negative parity and $I=1$, 2, or 3 for the 146-keV state. Since the γ intensity of the 146.2-keV line is an order of magnitude weaker than the 87.2-keV transition, it is inferred that the 146.2-keV transition is pure $E2$ and that the 146-keV level has $I^\pi=3^-$. The spin alternatives 1 and 2 would allow a magnetic dipole admixture in the 146.2-keV line. One would expect, therefore, that the intensity of the 146.2-keV line would be at least comparable to that of the 87.2-keV transition. This is in contrast with the observed intensities; consequently, $I^\pi=3^-$ is favored for the 146-keV level.

Instead of the above mode of de-excitation, one might consider the possibility that the 86.84-keV transition depopulates the 146-keV level. This transition energy is also consistent with the charged-particle

[36] G. Alaga, Nucl. Phys. **4**, 625 (1957).

reaction results and the high-energy (n,γ) data. Furthermore, the $M1$ character of this line would yield $I^\pi=1^-$, 2^-, or 3^- for the 146-keV state. The intensity of the 86.8-keV transition is, however, smaller than that expected from a statistical consideration of the de-excitation of the compound system. For this reason, it is improbable that the 146-keV level is depopulated through the 86.8-keV transition.

The adopted de-excitation mode of the 146-keV state suggests that this level be interpreted as the 3^- rotational member of the ground-state band. Computing the rotational parameter $\hbar^2/2\mathcal{I}$ from the experimentally observed energy of the 2^- member of the ground band, a value of 147.522 keV is calculated for the position of the 3^- level. This energy is 1.25 keV above the experimental level energy, and indicates that the ground-state rotational band probably experiences a high degree of mixing. It is noteworthy that the discrepancy would increase if the 86.8-keV transition were to be considered as depopulating the 146-keV level. On the basis of Alaga's rule, one can calculate the $E2$ admixture in the 87.2-keV transition using the branching ratio of the 87.2- and 146.2-keV lines. The result I_γ ($E2$, 87.2 keV) $=(5\times10^{-3})\times I_\gamma$ (87.2 keV) is consistent with the internal conversion data ($M1+<4\%$ $E2$).

5. 4^- *Level at* 173 *keV*

This level is established through the high-energy (n,γ) data which yield an excitation energy of 73.9 ± 1.1 keV above the 99-keV state. Two modes of de-excitation of the 173-keV level are compatible with this excitation energy (173.2 ± 1.1 keV): (a) a 174.271-keV $M1$ ground-state transition or (b) a 74.568-keV $M1+E2$ line leading to the 99-keV level. In either case, negative parity is required for the 173-keV level.

In the first case, the 174.27-keV state would have a spin-parity assignment of 1^- or 2^-, because of the $M1$ character of the depopulating transition and the intensity of the primary γ-ray line. The level would then have to be interpreted as a $K^\pi=1^-$ or $K^\pi=2^-$ band head. In view of the possible Nilsson configurations available to form such a band at this excitation energy, it seems unreasonable that the band head would decay only to the ground state. No transition to the 59- or 99-keV levels has been observed; hence, it is believed that the 173-keV state does not decay in this mode.

The depopulation through the strong 74.568-keV transition to the 99-keV level is most easily understood if one interprets the 173-keV state as the $K^\pi=4^-$ band head of the $p[402\uparrow]$; $n[512\downarrow]$ configuration. The possibility that the 173-keV level is the 4^- rotational member of the $K^\pi=3^-$ band at 99 keV seems improbable, because a possible $E2$ transition to the 2^- rotational member of the ground-state band is not observed.

The conversion electron data and the $I^\pi=3^-$ structure of the 99-keV state imply $I^\pi=2^-$, 3^-, or 4^- for the 173-keV level. In the (d,p) and (d,t) spectra, this level is observed as part of an unresolved doublet. The complex nature of this line is revealed through the (d,p) exposures at 35° and 45°. At these angles, the spectrograph resolution was somewhat better than at other angles, and the line appeared to be partially resolved. The charged-particle reaction data further indicate that the (d,t) complex group is shifted to lower excitation energies, which implies that the lower-lying component ($E_{exc}\simeq173$ keV) has more hole character. In view of the degree of (d,t) population of the 1^-, 2^-, and 3^- members of the ground-state rotational band, these observations support the I^π, $K=4^-$, 4 assignment of the 173-keV level.

6. 6^- *Level at* 186 *keV*

The (d,p) and (d,t) data suggest that this level is the upper member of the complex group centered at 180 keV in the (d,p) spectrum, and discussed briefly in Sec. III A 5. The proton angular distribution of this group indicates that the $l=3$ component dominates. The shift of the complex line in the (d,t) data as compared with the (d,p) results suggests that the upper component ($E_{exc}\approx186$ keV) has predominantly particle character.

The experimental cross section and angular distribution of this complex group can well be explained if one assumes that the 186-keV state is the $K^\pi=6^-$ band head of the $p[402\uparrow]$; $n[503\uparrow]$ configuration. This state is expected to be fed in the (n,γ) process through secondary and higher-order γ cascades. Its de-excitation can occur to the 3^- member of the ground-state rotational band through a twice-K-forbidden, 40-keV, $M3$ transition, to the 99-keV level through an 86-keV, $M3$ line, and to the 173-keV state through an $E2$ transition with an energy of approximately 12 keV.

In Re^{188} the decay of the 6^- isomer has been studied in detail by Takahashi *et al.*[37] These authors found the isomer to be populated with $I_\gamma\approx1.8/100n$, and they also observed that the $M3$ transitions depopulating the isomer are hindered by factors of the order of 100–2000. Assuming that the situation in Re^{111} is similar to that in Re^{188}—except for transition energies—we would expect that the 40-keV transition is very weak compared with the 86-keV line. Thus the 6^- level would have a half-life of the order of 3 sec. No such isomer has been observed. Therefore, it is interesting to consider the effect of the 12-keV, $E2$ transition. The Moszkowski estimate for this transition is $(t_{1/2})_\gamma\approx10^{-2}$ sec. Since the total conversion coefficient of a 12-keV line in rhenium is of the order of 10^5, the expected partial half-life would be approximately

[37] K. Takahashi, M. McKeown, and G. S. Goldhaber, Phys. Rev. **136**, B18 (1964).

0.1 μsec. This value is, of course, quite uncertain because of the lack of knowledge of the transition energy and the actual hindrance.

It is interesting to note that Brandi *et al.*[38] have observed a 70-μsec isomer in Re^{186}. These authors found that K x rays are primarily emitted during the depopulation of the isomer. Additionally, weak lines with energies of 99 and 128 keV, which were tentatively assigned to the isomeric decay, were observed. The intensity ratios $I(K\text{ x}):I(99\text{ keV}):I(128\text{ keV})=80:1:1$ were also reported and coincidences between K x rays were observed. If it is assumed that the Re^{186} 6^- isomer is depopulated only through the 12-keV, $E2$ transition leading to the 173-keV state, the ratio $I(K\text{ x}):I(99\text{ keV})=57:1$ is predicted. To obtain this result, the fluorescence yield has been taken as unity, and the 59-keV γ radiation has been added to the intensity of the K x radiation resulting from the conversion of the 99- and 74-keV lines. The coincidence between K x-ray quanta as observed by Brandi *et al.* would then be due to the coincidence between the 74- and 59-keV transitions. Unfortunately, these authors were not able to isolate the K x rays from the 59-keV radiation. Although the preceding considerations do not contradict the assignment of the 6^- state, there appears no explanation for the 128-keV transition observed by Brandi *et al.*

7. 2^- *Level at* 210 *keV*

A level at this energy is populated through the (d, p) and (d, t) reactions, and through a primary γ-ray transition. Independently, the level is established through a series of loops using low-energy transitions. On the basis of the spin-parity assignments discussed previously, $I^\pi=2^-$ is obtained for this level. The shape of the proton angular distribution, together with the magnitude of the (d, p) and (d, t) cross sections, suggests that this state is the $K^\pi=2^-$ band head of the $p[402\uparrow]$; $n[510\uparrow]$ configuration.

The branching ratio of the transitions depopulating the 210-keV level to the ground-state band do not obey the simple Alaga rule. This observation indicates that the $K^\pi=2^-$ band is probably mixed with the $K^\pi=1^-$ ground-state band, and with the $K^\pi=3^-$ band at 99 keV.

8. 4^- *Level at* 268 *keV*

The most intense primary γ ray populates a level at 268.4 ± 1.0 keV. The transitions de-exciting this state should have an intensity sum greater than $1.2/100n$. Within the uncertainty of 1.0 keV, the 268.4-keV state is obtained through the following low-energy transitions: a 122.525-keV line leading to the 146-keV, 3^- level; a 169.431-keV, $E2$ transition feeding the 99-keV, 3^- state; and a 209.82-keV line to the 2^- state at 59 keV. However, only the 169.431- and 122.525-keV transitions form an acceptable energy loop within the uncertainties quoted for the low-energy transitions. Using these transition energies, the resulting level has an energy of 268.796 ± 0.011 keV and negative parity because of the $E2$ multipolarity of the 169.4-keV line. The 209.8-keV transition may represent a depopulation of the 268-keV level, but this is not as certain because the transition energy is greater than the level-energy difference by about 1.5 the standard deviation.

From the preceding considerations, the 268-keV level has the following spin possibilities: $I^\pi=2^-$, 3^-, or 4^-. However, since there is no evidence for a ground-state transition, $I^\pi=4^-$ is favored.

Fitting the first three members of the ground-state rotational band to the formula

$$E_{1,I}=E_1{}^0+A_1[I(I+1)]+B_1[I^2(I+1)^2],$$

the values $E_1{}^0=-29.8$ keV, $A_1=14.95$ keV, and $B_1=-0.022$ keV are obtained. Using these parameters, the 4^- member of the ground-state rotational band is calculated to lie at approximately 264.4 keV. This result is approximately 4.4 keV below the experimentally observed energy of the $I^\pi=4^-$ level. Nevertheless, in view of the possibilities of mixing, it does not appear unreasonable to consider the 268-keV state as the 4^- rotational member of the ground-state band. Although the simple rotational model does not reproduce the level energy very well, the interpretation is consistent with the $E2$ multipolarity of the 169.4-keV radiation, since the $M1$ component of this γ line would be once K-forbidden. Furthermore, if the 209.8-keV transition does in fact depopulate the 268-keV level, a comparison of the γ branching ratio of the 122.5- and 209.9-keV lines with the branching ratio of the 87.2- and 146.2-keV transitions can be made. Assuming that the reduced magnetic dipole and reduced electric quadrupole transition probabilities are given by

$$B(M1)\propto C^2\,|\,\langle I_i 1K0\,|\,I_f K\rangle\,|^2$$

and

$$B(E2)\propto q^2\,|\,\langle I_i 2K0\,|\,I_f K\rangle\,|^2,$$

the ratio q^2/C^2 can be calculated by using the γ intensities of the 87.2- and 146.2-keV transitions and Alaga's rule for the computation of the $E2$ admixture in the 87.2-keV line. In the adiabatic approximation, q^2/C^2 should be a constant within a band. Using this ratio and assuming that the 122.5- and 209.8-keV transitions have $M1$ and $E2$ multipolarity, respectively, the result

$$I_\gamma(122\text{ keV})/I_\gamma(209\text{ keV})=4.3$$

is obtained. This value agrees well with the observed value of 4.0. These considerations are consistent with the structure proposed for the 268-keV level. However, we still prefer to regard the assignment as tentative.

[38] K. Brandi, R. Engelmann, V. Hepp, E. Kluge, H. Krehbiel, and U. Meyer-Berkhout, Nucl. Phys. **59**, 33 (1964).

9. 4^- *Level at* 273 *keV*

This level is strongly populated in the (d, p) and (d, t) experiments. Independently, it is obtained through energy combinations of low-energy γ lines. Intense transitions feed the levels at 173, 146, and 99 keV, which have $I^\pi = 4^-$, 3^-, and 3^-, respectively. The observed multipolarities of the 127.3- and 174.2-keV transitions are consistent with $I^\pi = 2^-$, 3^-, or 4^- for the 273-keV level. In view of the structure proposed for the 1^- ground state, the 59-keV 2^- level, and the 146-keV 3^- state, one would expect transitions to the 1^- and 2^- states if the spin of the 273-keV level were 2^- or 3^-. These transitions are not observed and we conclude that the level has $I^\pi = 4^-$.

Based on model assumptions, the 273-keV level is believed to be the 4^- rotational member of the $K^\pi = 3^-$ band at 99 keV. The large (d, p) and (d, t) cross sections of this level, in conjunction with the fact that the proton angular distribution appears dominated by $l = 1$–3, support the proposed assignment.

10. 3^+ *Level at* 314 *keV*

This level is obtained through energy combinations using intense low-energy γ transitions. The multipole character of these transitions implies positive parity and, on the basis of the spin assignments previously discussed in the text, $I = 2$ or 3. The fact that no ground-state transitions have been observed, together with the existence of strong transitions to the 2^- and 3^- levels of the ground band, favors spin 3 for the 314-keV level. Spin 2, however, cannot be excluded.

Three interpretations of the 314-keV level are possible:

(1) $p[402\uparrow]; n[615\uparrow]$,

(2) $p[402\uparrow]; n[651\downarrow]$,

and

(3) $p[514\uparrow]; n[512\downarrow]$.

The first possibility presents itself because the $[615\uparrow]$ configuration is most probably observed as the 257-keV isomeric state in Os^{187}.[4] This alternative is excluded, however, since $E1$ depopulation to the configurations already mentioned in connection with the low-lying levels in Re^{186} would be very strongly hindered. This is not experimentally observed.

The $K^\pi = 2^+$ band head generated from configuration 2 is also a possible assignment. The experimental $B(E1)$ value for a transition between the 314-keV level and the 2^- (or 3^-) member of the ground-state band is a factor of 5 smaller than for a similar transition to the $K^\pi = 2^-$ (or $K^\pi = 3^-$) band head. These $B(E1)$ values are difficult to understand in terms of configuration 2 and in light of the configurations proposed for the ground, 99-, and 210-keV states. Furthermore, the $K^\pi = 2^+$ band head formed from configuration 2 should have a moderately intense (d, p) cross section. It has not been possible to detect such a level in the charged-particle reaction experiments.

In Re^{187} an 0.56-μsec isomer occurs with an energy of 206.4 keV and has been interpreted as arising from the $p[514\uparrow]$ configuration.[4] From the Nilsson scheme[39] it is clear that a small change in deformation should not drastically alter the relative separation of the $p[402\uparrow]$ and $p[514\uparrow]$ orbitals. Therefore, from a consideration of the systematics of the $p[514\uparrow]$ orbital, the state at 314 keV in Re^{186} may be interpreted as the $K^\pi = 3^+$ band head of the $p[514\uparrow]; n[512\downarrow]$ configuration. With this interpretation, the odd proton is an excited quasiparticle and this is consistent with the observation that the 314-keV level is not appreciably populated in the charged-particle reaction experiments. By contrast, the relatively large value of $B(F1)$ for the transitions to the $K^\pi = 2^-$ and $K^\pi = 3^-$ band heads cannot be easily explained in terms of configuration 3. These anomalous transition rates may find their explanation in mixing with higher- and/or lower-lying two-quasiparticle excitations. From the discussion of the possible interpretations of the 314-keV level, we believe configuration 3 to be most probable. In Fig. 6 the configuration is enclosed in parentheses, indicating that the assignment is tentative.

Berestovoy *et al.*[11] have studied delayed coincidences from the reaction $Re^{185}(n, \gamma)$ and found $t_{1/2} = 11.8$ nsec for a spectrum containing lines with energies 62 ± 3, 100 ± 4, 142 ± 3, 210 ± 4, and 255 ± 6 keV. All of these lines except for the intense 142-keV transition appear to be emitted during the de-excitation of the 314-keV level. Because of the intensity of the 142-keV line relative to the intensities of the other hindered transitions, these authors conclude that the 142-keV line is an isomeric transition which proceeds from the isomer at 458 keV to the 314-keV level. The 142 ± 3-keV hindered line that they observe most probably corresponds to the intense 144.152-keV, $E1$ transition observed in the present investigations. On the basis of the $E1$ multipolarity, the 458-keV level proposed by Berestovoy *et al.* has $I^\pi = 2^-$, 3^-, or 4^- and should be a band head. It is surprising, then, that this 458-keV level decays only to the 314-keV state and to no other level. If one considers the 314-keV level to be the 11.8-nsec isomer, the half-life of the 142-keV transition is unexplained. Although it is believed that the 314-keV level has predominantly the structure $p[514\uparrow]; n[512\downarrow]$, it is not possible, on the basis of the present experimental data, to identify the 11.8-nsec isomer.

11. 1^- *Level at* 316 *keV*

The energy difference between the very intense 316.473 ± 0.020-keV line and the strong 257.446 ± 0.015-

[39] A. Faessler and R. K. Sheline, Phys. Rev. **148**, 1003 (1966).

keV transition is 59.027±0.025 keV, which agrees well with the spacing (59.009±0.004 keV) between the 2^- and 1^- members of the ground-state band. This energy combination serves to establish this level. The $M1$ multipolarities of the 257.4- and 316.4-keV transitions imply that this state has $I^\pi=1^-$ or 2^-. No strong transitions to lower-lying states with $I^\pi=3^-$ or 4^- have been observed. A possible weak line to the 99-keV, 3^- state coincides in energy with a Re^{188} transition; another very weak transition with energy 170.185 keV to the 146-keV, 3^- level might constitute part of the complex peak centered at 170.47 keV; and a 105.764-keV line to the 2^- level at 210.6 keV cannot be isolated from the tail of the strong 105.86-keV line of Re^{188}. These facts and, in particular, the weak strengths of the transitions to the spin-3 levels, suggest that the 316-keV level has $I=1$. The absence of a lower-lying 0^- state indicates that the 316-keV level is probably the $K^\pi=1^-$ band head of the $p[402\uparrow]$; $n[503\uparrow]$ configuration. The predicted branching ratio (1.86) of the 316- and 257-keV transitions agrees well with the experimental result of 1.77±0.25.

12. 3^- *Level at 322 keV*

The high-energy γ-ray transition with energy 5857.8 keV feeds a level at 321.7±1.5 keV. This state is also strongly excited in the (d, p) and (d, t) reactions, but a possible weak population of the 316-keV state probably causes a shift of the line toward lower excitation energies. Allowing for the intensity of the primary γ ray, and assuming a reasonable estimate for the population through γ-ray cascades, the de-excitation mode of the 322-keV state can be inferred. The primary γ-ray line implies $1\leq I\leq 4$ for the 322-keV level, and the population through γ-ray cascades is expected to be $I_\gamma+I_e\approx 4/100n$, as can be seen from the populations of the other $I=4$ states previously discussed. The deexcitation mode which is indicated in the level scheme (Fig. 6) appears to be the only choice consistent with the population and energy requirements of the 322-keV level. The multipole character of the 223.0-keV transition implies negative parity for this level. Spin 3 is strongly suggested because of the de-excitation mode and the absence of a reasonably intense 322.39-keV ground-state transition. The preferential decay of the 322-keV state to the level at 210 keV, together with the magnitude of the (d, p) and (d, t) cross sections of the 322-keV level, indicates that this state is probably the $I^\pi=3^-$ rotational member of the $p[402\uparrow]$; $n[510\uparrow]$, $K=2$ band.

Calculating the energy of the 322-keV level through combinations with low-energy γ-ray lines, we find that the 111.674-keV transition does not fit between the 322- and 210-keV states within the statistical energy error (6 eV; Table III, column 2). The discrepancy is 20 eV, which is more than seems tolerable. According to the above interpretation of the 322-keV level, one expects the 111.6-keV line to be predominantly an $M1$ transition. Unfortunately, in the conversion electron measurements, it was not possible to resolve the 111.6- and 111.8-keV lines. However, if one assumes the 111.6-keV transition to be $M1$, then the total K and L conversion electron intensity is not consistent with either an $E1$, $U2$, or $M1$ multipolarity assignment for the 111.8-keV transition. Therefore, it is believed that the 111.6-keV line is a doublet where one component proceeds between the 322- and 210-keV levels. This would also be in better agreement with the population considerations of the 322-keV state. For these reasons, the 111.6-keV transition has been included as a dashed line in the level scheme (Fig. 6).

13. 2^- *Level at 378 keV*

This state is weakly fed through a primary γ line and is also weakly populated in the (d, p) and (d, t) reactions. Its depopulation occurs through four low-energy lines with medium-large intensities. The multipolarity of the 61.928- and 232.100-keV transitions determines the spin-parity assignment of the 378-keV level as 2^-. The high γ intensity of the 61.9-keV line implies that the 378-keV level can be reasonably interpreted as the 2^- rotational member of the $p[402\uparrow]$; $n[503\uparrow]$, $K=1$ band. This assignment is supported by the (d, p) angular distribution. Furthermore, the ratio of the (d, p) and (d, t) cross sections indicates that the 378-keV level is predominantly a particle state. This behavior is expected of the $[503\uparrow]$ neutron orbital. The experimentally observed branching ratio is

$$I_\gamma(378\text{ keV}):I_\gamma(319\text{ keV}):I_\gamma(232\text{ keV})=3.8:1.0:1.3,$$

which is in good agreement with the predicted ratio 3.0:1.0:1.3 for $M1$ radiation.

14. 4^- *Level at 469 keV*

The 469-keV level is populated directly through a primary γ transition after slow neutron capture by Re^{185}. It is strongly fed in the (d, p) and (d, t) reaction, and it most probably decays through three γ transitions to the 322-, 268-, and 173-keV levels. This deexcitation mode implies negative parity and $I=3$ or 4 for the 469-keV state. The large intensity of the 147-keV depopulation to the 322-keV level suggests that the 469-keV state may be the 4^- rotational member of the $p[402\uparrow]$; $n[510\uparrow]$, $K=2$ band. This interpretation is consistent with the energy sequence of the $I^\pi=2^-$, 3^-, and 4^- levels in this band. The experimentally observed charged-particle cross sections are, however, considerably larger than expected for the unmixed configuration.

15. 5^- *and* 6^- *Levels of the Ground-State Rotational Band*

The transitions deexciting the $I^\pi=2^-$, 3^-, and 4^- levels of the ground-state band are fairly strong. Popu-

lation considerations[40] indicate that the total depopulation of the 5^- member of the ground band should be $I_\gamma+I_n\approx(1/100\text{–}2/100)n$. Therefore, it should be possible to find the strongest γ lines which depopulate the 5^- level among the lines listed in Table III. The transitions proceeding to the 4^- and 3^- members of the ground-state rotational band must then satisfy the following conditions: (a) The energy combination must be satisfied; (b) the sum of their total intensities should be of the order of (1/100–2/100) counts, if the intensities of possible transitions to the 99-, 174-, and 273-keV levels are neglected; (c) their branching ratio should be of the order of $(1/100\text{–}2/100)n$, if the intensities of possible transitions to the 99-, 173-, and should follow the systematics within a rotational band; and (d) their observed multipolarities must agree with the expected multipole character. It is also required that the parameter $A_I=\hbar^2/2\mathcal{I}$ computed from the energy of the 5^- rotational member be comparable to the parameters obtained from the other members in the band. For the ground band, the parameters A_I calculated from the energy separations of the levels I and I-1 are $A_2=14.75$ keV, $A_3=14.55$ keV, and $A_4=15.32$ keV.

The 148.994- and 271.47-keV transitions meet all the requirements indicated above. The energy combination principle is satisfied within less than half the energy error; the total intensity of both lines is about $1.7/100n$; the experimental branching ratio $I_\gamma(148\text{ keV})/I_\gamma(271\text{ keV})=2.5\pm0.6$ agrees with the expected ratio of 2.0; the multipole character of the 148-keV line yields the correct parity of the state; and the excitation energy of the level fits nicely into the predicted rotational energy sequence. The value $A_5=14.90$ keV is obtained for the rotational parameter; consequently, the level is tentatively considered as the 5^- rotational level of the ground band.

In a speculative manner one can now proceed to look for transitions depopulating the 6^- rotational state. The 179.448- and 328.42-keV transitions are candidates which satisfy the energy combination principle. The expected branching ratio $I_\gamma(179\text{ keV})/I_\gamma(328\text{ keV})=4.1$ agrees well with the observed ratio of 3.9. The rotational parameter $A_6=14.95$ keV supports the assumption that the transitions are intraband transitions de-exciting the 6^- member of the ground-state rotational band. Also, the γ-intensity sum of the lines ($I_\gamma=0.34$) has a reasonable magnitude. The 6^- member at 597 keV, however, should not be considered as well established.

16. 3^- *Level of the Band at* 316 *keV*

A state at 470 keV is indicated through several loops. The strongest line is the 92.122-keV transition and is observed to have an $M1$ multipolarity. It leads to the 378-keV level which decays through an intense 61.9-keV, $M1$ transition to the 316-keV state. This latter decay implies that the intraband transition (61.9-keV line) is relatively fast compared with the interband transitions leading to levels in the ground-state rotational band. Assuming that the same holds for the de-excitation of the 3^- member of the 316-keV band, it may be identified with the 470.507-keV state. All other transitions depopulating the 470-keV level feed states with reasonable spins. The sequence of level energies 316.463, 378.383, and 470.507 keV agrees well with what is expected for a rotational band. In spite of these facts, we prefer to regard the 470-keV level as tentative.

17. 680-*keV Level*

This state is suggested through the energy combination principle. There is evidence that it decays to the ground state via the 680.0-keV line, to the 59-keV level through the 621.0-keV line, to the 99-keV state via the 580.3-keV transition, to the 146-keV state through the 533.9-keV transition, to the 210-keV state through the 469.3-keV line, to the 322-keV level via the 357.6-keV line, and to the level at 316 keV via the 363.4-keV transition. The decay of this level occurs to states with $I^\pi=2^-$, 3^-, and 4^-, and all loops close well within the energy uncertainty of the lines. In view of accidental combinations and the large energy errors, however, the level at 680 ± 0.10 keV should not be considered as well established.

B. Angular Distributions

The differential cross section for a deuteron stripping reaction on a target with total angular momentum I_i may be written[41]

$$\frac{d\sigma}{d\Omega}=B\sum_{j,l}S_{j,l}\Phi_l(\theta), \tag{2}$$

where $B=(2I_f+1)/(2I_i+1)$; I_f is the total angular momentum of the final state; l and j are the orbital and total angular momentum, respectively, of the captured neutron; $S_{j,l}$ is the spectroscopic factor which expresses the overlap between the initial state plus one neutron and the final nuclear state; and $\Phi_l(\theta)$ is the single-particle differential cross section. The spectroscopic factor can be written in terms of the reduced-width amplitude $\Theta_{j,l}$ as $S_{j,l}=\Theta_{j,l}^2$. For an odd-odd residual nucleus, if one assumes a single-particle model where two nucleons are strongly coupled to a deformed core, one can express the reduced-width amplitude as[42]

$$\Theta_{j,l}=B^{-1/2}\langle jI_i\Omega_\nu K_i \mid I_fK_f\rangle\langle\phi_f\mid\phi_i\rangle C_{j,l}^{\Omega_\nu}(U_\nu^2)^{1/2}$$

if $K_f=K_i+\Omega_\nu$, as

$$\Theta_{j,l}=B^{-1/2}(-1)^{j-\Omega_\nu}\langle jI_i-\Omega_\nu K_i \mid I_fK_f\rangle \times\langle\phi_f\mid\phi_i\rangle C_{j,l}^{\Omega_\nu}(U_\nu^2)^{1/2} \tag{3}$$

[40] O. W. B. Schult, B. P. Maier, H. R. Koch, and H. Gruber, Z. Physik **185**, 295 (1965).

[41] M. H. Macfarlane and J. B. French, Rev. Mod. Phys. **32**, 567 (1960).

[42] We wish to thank Dr. T. Udagawa for making these relationships available to us.

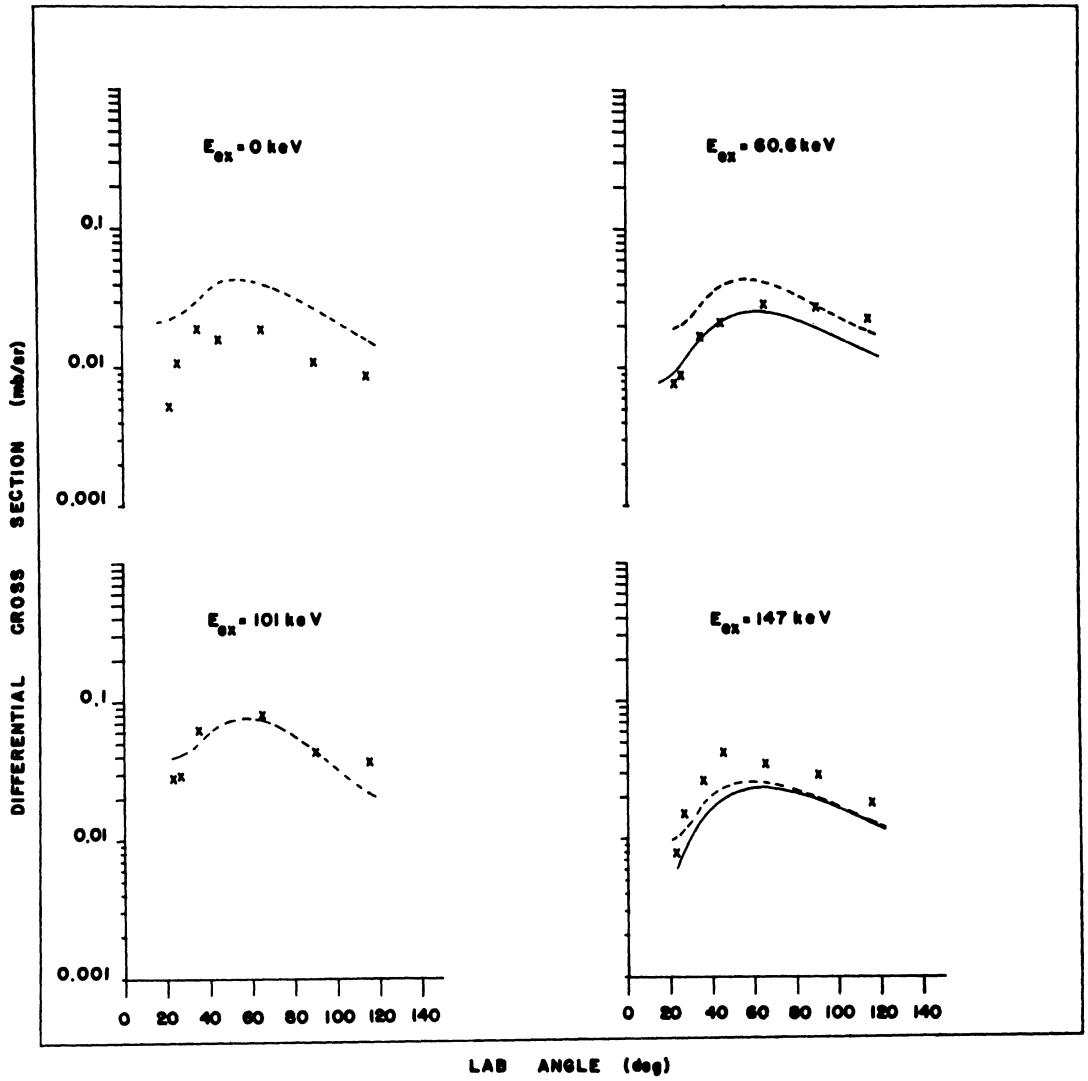

FIG. 7. Angular distributions for the 0-, 60.6-, 101-, and 147-keV proton groups. The crosses represent experimental data points. An experimental point at 45° for the 101-keV distribution is not plotted, because it was obscured by an impurity. Dashed lines indicate the theoretical angular distribution calculated on the basis of the spin-parity assignments given in Sec. III A. Where the Coriolis interaction has significantly changed the angular pattern, a solid line representing the theoretical angular distribution after these mixing effects have been considered is also plotted. Pairing effects have been included in all calculations.

if $K_f = K_i - \Omega_\nu$, or as

$$\Theta_{j,l} = B^{-1/2}(-1)^{I_i+K_i}\langle jI_i\Omega_\nu - K_i \mid I_fK_f\rangle \times \langle\phi_f \mid \phi_i\rangle C_{j,l}^{\Omega_\nu}(U_\nu^2)^{1/2}$$

if $K_f = \Omega_\nu - K_i$, where K_i and K_f represent, respectively, the projections of the initial- and final-state total angular momentum on the nuclear symmetry axis; Ω_ν is the projection of the total angular momentum of the captured neutron on the symmetry axis; $C_{j,l}^{\Omega_\nu}$ is the amplitude in an expansion of the deformed neutron single-particle wave function in terms of the spherical limit eigenfunctions $\psi_{j,l}^{\Omega_\nu}$; $\langle\phi_f \mid \phi_i\rangle$ is the overlap of the initial and final vibrational states; and U_ν^2 is the occupation probability associated with the intrinsic neutron single-particle orbit. For levels which lie well below the energy gap, it is usually assumed that $|\langle\phi_f \mid \phi_i\rangle|^2 = 1$. When this assumption is valid, the angular dependence of $d\sigma/d\Omega$ can be regarded as residing solely in the $\Phi_l(\theta)$ term.

Because of the presence of the sum operator in Eq. (2), the (d, p) angular distribution of any arbitrary state in an odd-odd deformed nucleus will not be characterized by a unique orbital angular momentum transfer. In addition, the angular distribution pattern will be affected if the final state contains ad-

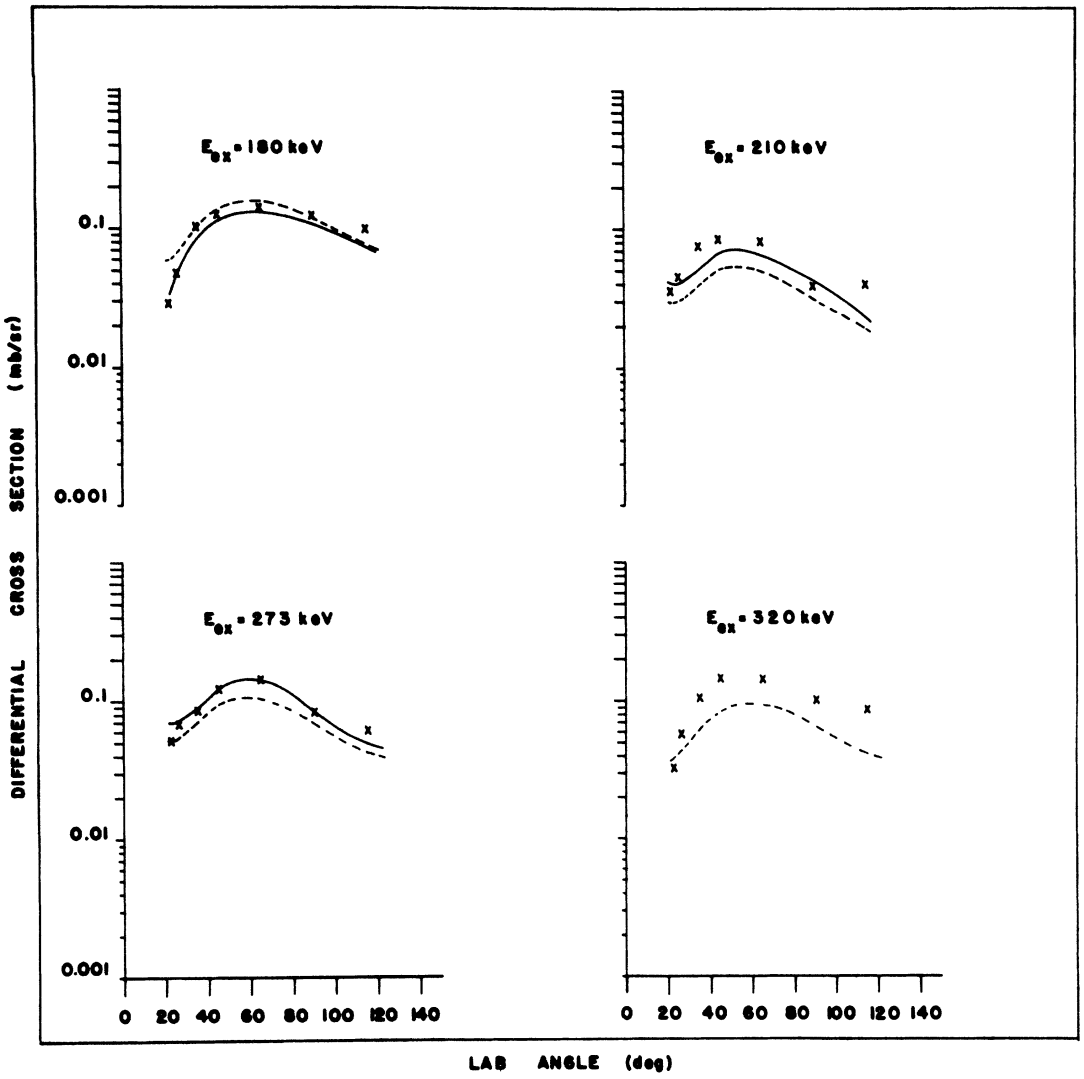

FIG. 8. Angular distributions for the 180-, 210-, 273-, and 320-keV proton groups (see Fig. 7 caption).

mixtures of other configurations. When there is mixing, the reduced-width amplitude must be modified to the form

$$\Theta_{j,l} = \sum_k a_k \Theta_{j,l,k}, \tag{4}$$

where a_k is the amplitude of the kth state in the final-state wave function. Therefore, in cases where mixing effects are large, the angular dependence of the differential cross section may significantly differ from that predicted by Eq. (2) with reduced-width amplitudes given by Eq. (3). Furthermore, the fact that each term in Eq. (4) may contain occupation probability coefficients of different magnitude must also be carefully taken into account.

For levels in the low-energy spectrum of Re^{186}, the theoretical angular distribution associated with each level is calculated on the basis of the spin, parity, and configuration given in Sec. III A. In Figs. 7–9, the experimental angular distributions are presented for many of the levels up to an excitation energy of 533 keV. Where a level has been assigned a spin, parity, and configuration, the appropriate theoretical angular distribution is plotted in the figure as a dashed line. If Coriolis coupling has significantly changed the initially calculated pattern, a solid line representing the theoretical angular distribution after these mixing effects have been taken into account is also plotted. The $C_{j,l}{}^{\Omega_p}$ coefficients (Table IV) employed in these calculations were obtained for a deformation $\beta = 0.22$ from a computer code based on the method of Faessler and Sheline.[39] The occupation probabilities used in these calculations are 0.55, 0.45, and 0.80 for the

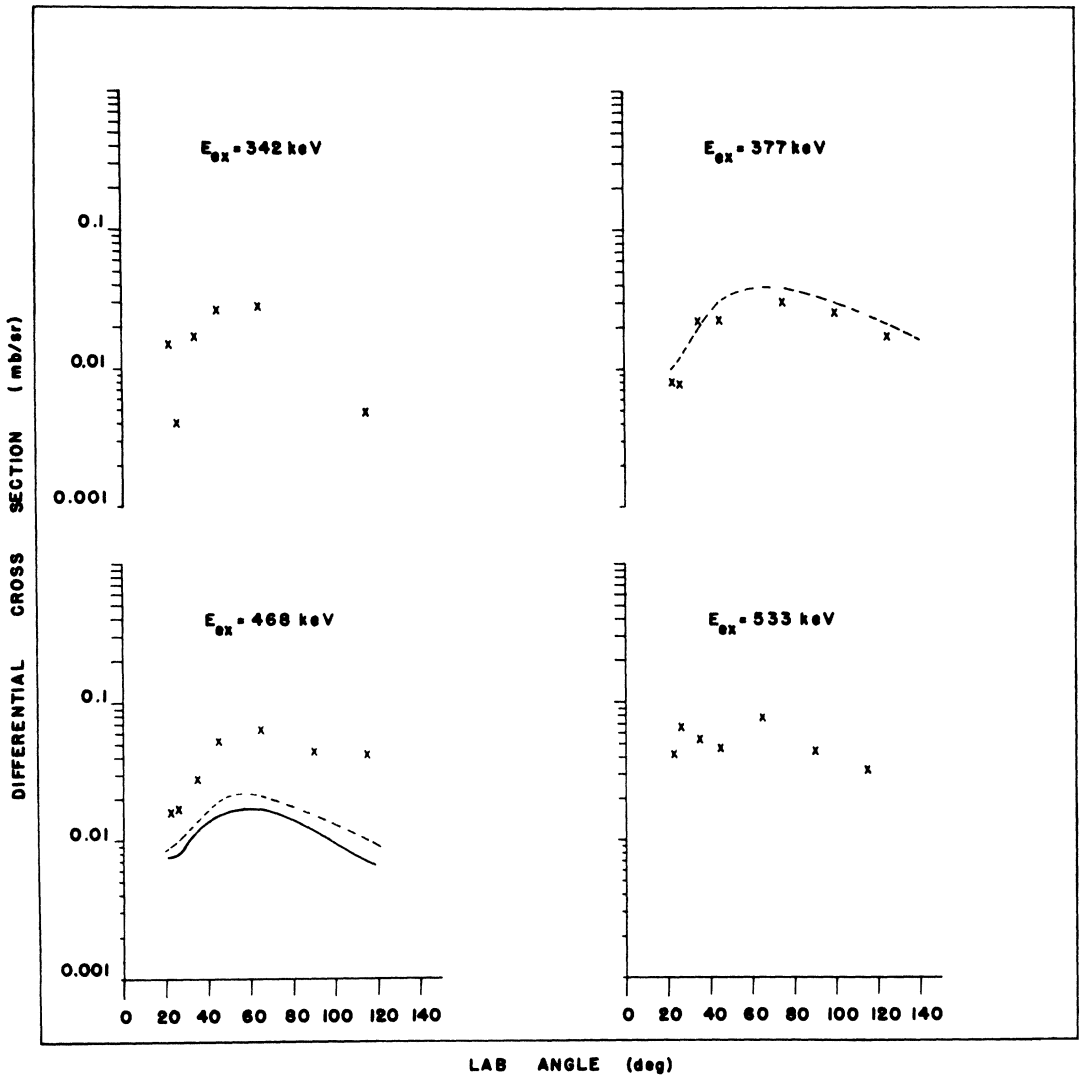

FIG. 9. Angular distributions for the 342-, 377-, 468-, and 533-keV proton groups (see Fig. 7 caption).

$[512\downarrow]$, $[510\uparrow]$, and $[503\uparrow]$ orbitals, respectively.[43] The theoretical single-particle angular distributions for Re^{186} were computed utilizing the T-SALLY[44] code with optical-model parameters[45] given in Table V. In obtaining the single-particle cross sections, no cutoff radius was employed.

Table VI completely summarizes the experimental and theoretical (d, p) cross sections for levels up to an excitation energy of 533 keV. The experimental absolute differential cross sections are probably reliable to about 30 or 40%. This large uncertainty is primarily due to uncertainties in the target thickness. A 15–25% uncertainty is a reasonable figure for the relative cross sections.

C. Band-Mixing Calculations

A Coriolis band-mixing calculation has been applied to some of the odd-A isotopes of tungsten and has been shown to account successfully for the observed (d, p) cross sections and γ-ray branching ratios.[46] Erskine and Buechner[47] have done a Coriolis-type cal-

[43] These values are estimates taken from a qualitative comparison of the (d, p) and (d, t) spectra.

[44] R. H. Bassel, R. M. Drisko, and G. R. Satchler, Oak Ridge National Laboratory Report No. ORNL-3240 (UC-34-Physics) (unpublished).

[45] The optical-model parameters are taken from Tables IV and V in R. H. Siemssen and J. R. Erskine, Phys. Rev. **146**, 911 (1966).

[46] R. T. Brockmeir, S. Wahlborn, E. J. Seppi, and F. Boehm, Nucl. Phys. **63**, 102 (1965); J. R. Erskine, Phys. Rev. **138**, B66 (1964); A. K. Kerman, Kgl. Danske Videnskab. Selskab, Mat.-Fys. Medd. **30**, No. 15 (1956).

[47] J. R. Erskine and W. W. Buechner, Phys. Rev. **133**, B370 (1964).

TABLE IV. $C_{j,l}^{\Omega_\nu}$ coefficients for the [512 ↓], [510 ↑], and [503 ↑] orbitals for $\beta=0.22$.

[512 ↓]			[510 ↑]			[503 ↑]		
j	l	$C_{j,l}^{3/2}$	j	l	$C_{j,l}^{1/2}$	j	l	$C_{j,l}^{7/2}$
			1/2	1	+0.0903			
3/2	1	−0.4997	3/2	1	+0.6461			
5/2	3	+0.7054	5/2	3	+0.5560			
7/2	3	+0.3364	7/2	3	−0.3691	7/2	3	+0.9342
9/2	5	−0.3629	9/2	5	−0.3477	9/2	5	+0.3298
11/2	5	−0.0891	11/2	5	+0.0899	11/2	5	−0.1362

culation in an attempt to explain the (d, p) spectrum of the odd-odd nucleus Ta^{182}. The Erskine-Buechner approach used Coriolis interaction matrix elements computed directly from Nilsson wave functions and gave a satisfactory fit to the experimental intensity patterns. It seemed worthwhile, therefore, to attempt a similar calculation for the levels in Re^{186}.

Levels having the same spin but with K quantum numbers differing by one unit ($|\Delta K|=1$) are expected to be coupled through the Coriolis force. The off-diagonal matrix element which expresses this coupling in an odd-odd nucleus is of the form[48]

$$\langle IMK+1 \mid H_{\mathrm{RPC}} \mid IMK\rangle = -[I(I+1)-K(K+1)]^{1/2} J_{K+1,K}, \quad (5)$$

where $J_{K+1,K}\equiv\langle K+1 \mid (\hbar^2/2\mathcal{I}) J_- \mid K\rangle$. In Re^{186}, therefore, Coriolis coupling among levels in the ground-state rotational band and bands having $K=2^-$, 3^-, and 4^- must be considered. For the spin-2, -3, and -4 levels of these bands, an extraction of the mixing amplitudes requires the diagonalization of matrices having dimensions 2, 3, and 4, respectively.

In making these band-mixing calculations, the off-diagonal matrix elements $J_{K+1,K}$ are parametrized. The diagonal matrix elements are given by

$$E_{K,I}^{0}=E_K^{0}+A_K[I(I+1)], \quad (6)$$

where $E_{K,I}^{0}$ represents the energy of an unperturbed level with projection quantum number K and spin I; E_K^{0} is the unperturbed band-head energy (relative to the ground-state band head which is not affected by the Coriolis interaction, since it cannot mix with any level included in these calculations); and A_K is the rotational parameter for the unperturbed system. For bands having the same intrinsic particle configuration, it is assumed that the unperturbed rotational pattern of these bands is characterized by the same moment of inertia. No attempt has been made to include rotation-vibration interaction effects on the rotational patterns of the observed bands.

TABLE V. Optical-model parameters utilized to compute the single-particle cross sections for the reaction $Re^{185}(d,p)Re^{186}$.

	V (MeV)	r_0 (F)	a (F)	W_D (MeV)	r_I (F)	a_I (F)
Deuteron	104.0	1.15	0.81	13.5	1.34	0.68
Proton	55.0	1.25	0.65	17.7	1.25	0.47

In lieu of a multiple parameter search to obtain the best fit to the experimental energies and cross sections, a more expedient and systematic method of calculation is employed. For the $I=2$ case, the necessary elements of the Hamiltonian matrix are calculated from the experimental energies and a reasonable choice of A_1. This calculation therefore fixes the values of A_1, $J_{2,1}$, and E_2^{0}. Using these values and the experimental $I=3$ energies, the necessary 3×3 Hamiltonian matrix is constructed, thereby fixing the additional parameters A_2, $J_{3,2}$, and E_3^{0}. Up to this point, then, five parameters are uniquely determined from a single choice of A_1 and five experimental energies.

Theoretically, $J_{2,1}=-J_{4,3}$; however, in these calculations we have taken $J_{4,3}$ as a free parameter. As a result, $J_{4,3}$ and E_4^{0} must be determined to complete the construction of the $I=4$ Hamiltonian matrix. Four equations in the two undetermined parameters result, and a least-squares procedure is employed to determine the best values for these parameters.

The three matrices obtained in this fashion are subsequently diagonalized and mixing amplitudes obtained. Using the values of U_ν^2 and the $C_{j,l}^{\Omega_\nu}$ coefficients referred to in Sec. III B, the differential cross sections of the mixed levels are calculated. This entire procedure is then repeated for a new choice of A_1.

The range over which A_1 is allowed to vary is restricted approximately to the values $19.0<A_1<24.0$ keV. These bounds are imposed because, for the calculation of $J_{2,1}$, $J_{3,2}$, and $J_{4,3}$, the appropriate equations contain the matrix elements of J quadratically. Hence, for the calculation to be entirely consistent among the three matrices, the square of these elements must be positive (otherwise the actual matrix element will be imaginary; this is not allowed on theoretical grounds). Only within the bounds given for A_1 is this situation

[48] G. L. Struble, J. Kern, and R. K. Sheline, Phys. Rev. **137**, B772 (1965).

TABLE VI. Summary of the (d,p) experimental and theoretical cross-section results. Columns labeled Expt contain the experimentally observed absolute cross sections (mb/sr); columns labeled Theor contain the theoretically calculated cross sections (mb/sr); columns labeled TB contain the theoretically calculated cross sections with band mixing and pairing effects included (mb/sr). Levels followed by asterisks (*) are treated as doublets in the cross-section calculations. A question mark (?) indicates that the level is either too weakly populated to be observed or that it is obscured by an impurity.

E_{expt}		22.5°			26.0°			35.0°			45.0°			65.0°			90.0°			115.0°		
(keV)	Expt	Theor	TB	Expt	Theor	TB	Expt	Theor	TB	Expt	Theor	TB	Expt	Theor	TB	Expt	Theor	TB	Expt	Theor	TB	Expt	Theor	TB
0.0	0.005	0.023	...	0.011	0.024	...	0.019	0.029	...	0.016	0.041	...	0.019	0.040	...	0.011	0.027	...	0.009	0.016	...			
60.6	0.008	0.019	0.009	0.009	0.020	0.010	0.017	0.028	0.016	0.022	0.039	0.022	0.028	0.041	0.025	0.028	0.029	0.019	0.023	0.018	0.013			
101	0.028	0.039	0.038	0.029	0.040	0.039	0.062	0.048	0.047	(?)	0.068	0.067	0.070	0.067	0.066	0.044	0.045	0.044	0.037	0.021	0.025			
147	0.008	0.010	0.006	0.015	0.011	0.008	0.026	0.017	0.014	0.042	0.023	0.019	0.035	0.026	0.024	0.029	0.020	0.019	0.018	0.013	0.013			
180*	0.029	0.053	0.036	0.047	0.059	0.042	0.105	0.100	0.084	0.127	0.136	0.112	0.147	0.158	0.138	0.127	0.122	0.112	0.100	0.080	0.076			
210	0.037	0.030	0.040	0.046	0.030	0.041	0.076	0.036	0.048	0.085	0.051	0.068	0.082	0.050	0.065	0.041	0.033	0.043	0.040	0.019	0.024			
273*	0.051	0.051	0.070	0.069	0.052	0.072	0.087	0.071	0.088	0.125	0.099	0.125	0.142	0.102	0.152	0.085	0.073	0.084	0.062	0.043	0.050			
320*	0.033	0.037	0.040	0.057	0.041	0.044	0.106	0.060	0.063	0.147	0.083	0.086	0.146	0.091	0.093	0.100	0.066	0.067	0.089	0.042	0.042			
342	0.015	...	...	0.004	...	...	0.017	...	...	0.027	...	...	0.018	...	...	(?)	...	...	0.005	...	...			
377	0.008	0.010	...	0.007	0.012	...	0.022	0.023	...	0.022	0.031	...	0.030	0.038	...	0.026	0.030	...	0.017	0.021	...			
414	0.004	...	...	0.006	...	...	0.010	...	...	0.003	...	...	0.027	...	...	0.011	...	...	0.017	...	...			
468	0.016	0.009	0.008	0.017	0.010	0.008	0.028	0.014	0.012	0.053	0.019	0.016	0.065	0.021	0.017	0.045	0.015	0.012	0.043	0.010	0.007			
533	0.042	...	...	0.067	...	...	0.052	...	...	0.047	...	...	0.078	...	...	0.044	...	...	0.032	...	...			

realized. It should be pointed out that these bounds are not guaranteed to be unique, because the calculation always assumed the same starting point, i.e., the calculation of the 2×2 matrix elements. Nevertheless, the assumption of a different starting point should not substantially change the main results of these calculations.

The parameters which appear to yield the best fit to the experimental intensity patterns are given in Table VII. Note that the wave functions listed for the 173.9- and 273.6-keV levels are in conflict with the assignments given in Fig. 6. Effects due to the rotation-vibration interaction become increasingly important for higher spin states and their inclusion would probably cause a substantial change in the wave functions of the $I=4$ levels.

Figure 10 graphically compares the experimental and theoretical (d, p) intensities for the low-lying levels in Re^{186} at 65° and 90°. The parameter $J_{3,2}$ given in Table VII is consistent with Erskine's determination of the $[510\uparrow]$ decoupling parameter in the odd-A tungsten isotopes[46] and indicates that there is little or no mixing of the $K^\pi=2^-$ and $K^\pi=3^-$ bands. By contrast, $J_{2,1}$, $J_{4,3}$, A_1, and A_2 differ by as much as 50% from Erskine's results. A calculation of the Re^{186} spectrum directly using the tungsten parameters (and the values of U_ν^2 given in Sec. III B) gave a somewhat poorer fit to the experimental level energies and (d, p) cross sections.

Although the inclusion of Coriolis coupling improves the fit to the experimental data, it is clear from Figs.

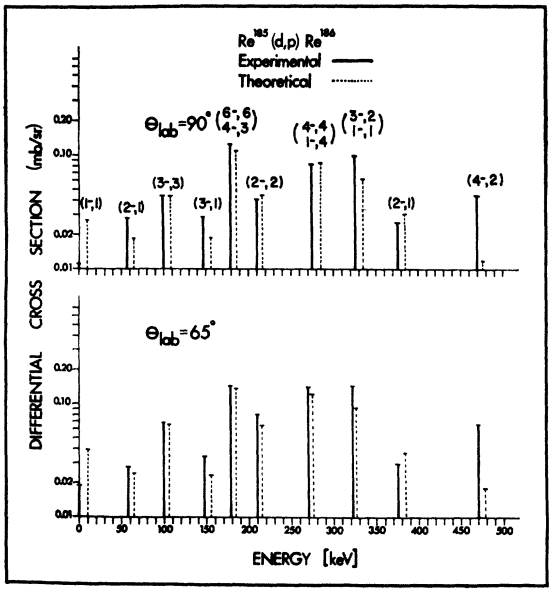

FIG. 10. Comparison of the experimental and theoretical cross sections for Re^{186} at 65° and 90°. The theoretical calculations include effects due to the Coriolis interaction and the pairing. The levels are labeled by I^π, K and the value of K given to each level is based on the results of the band-mixing calculation (Table VIII).

TABLE VII. Parameters and wave functions used in calculating cross sections of Coriolis mixed levels (see text for symbol definitions).

$A_1 = 19.22$ keV $A_2 = 13.94$

$E_2^0 = 192.82$ keV $E_3^0 = 99.36$ keV $E_4^0 = 241.63$ keV

$J_{2,1} = 24.46$ keV $J_{3,2} = +0.227$ keV $J_{4,3} = -16.72$ keV

		Wave function			
E_{expt}	E_{calc}	a_1	a_2	a_3	a_4
		$I=2$			
59.009	59.009	−0.9392	+0.3433		
210.696	210.696	−0.3433	−0.9392		
		$I=3$			
99.361	99.361	+0.0049	−0.0041	+0.9999	
146.275	146.275	−0.8597	+0.5108	−0.0061	
322.391	322.391	−0.5108	−0.8597	+0.0022	
		$I=4$			
173.929	176.52	−0.0028	+0.0046	+0.8091	+0.5876
268.796	261.11	−0.7738	+0.6331	+0.0083	−0.0202
273.628	275.98	−0.0177	+0.1194	−0.5876	+0.8089
469.795	472.83	−0.6332	−0.7740	+0.0026	−0.0007

7–10 that discrepancies still exist. In particular, the experimental intensity signature of the first three rotational members of the ground-state band is in disagreement with that predicted by theory. Furthermore, large deviations between experimental and predicted cross sections are also conspicuous for the 316-, 322-, and 469-keV levels.

The extremely weak strength of the ground state is particularly disturbing. Theoretically, no Nilsson configuration can give rise to a level sufficiently low in energy to mix with the ground state through the Coriolis force. From calculations in the region $160 < A < 180$, Soloviev[49] has shown that vibrational admixtures in low-lying two-quasiparticle states of odd-odd deformed nuclei are of appreciable significance. Because the γ-vibrational band becomes increasingly lower in energy for even-even nuclei near the region[50] $A = 186$, it is expected that these vibrational admixtures in Re^{186} will play an even greater role. The presence of vibrational admixtures could easily account for the weak strength of the ground state; however, the cross sections of the other rotational partners should also show a corresponding decrease in intensity. This is not observed.

In studies involving the reaction $W^{182}(d, p)W^{183}$, Siemssen and Erskine[51] have pointed out the existence of certain ambiguities regarding single-particle cross sections obtained from existing distorted-wave Born-approximation (DWBA) codes. Experimental spectroscopic factors for rotational levels built on the $[512\downarrow]$ and $[510\uparrow]$ neutron configurations are consistently larger (by about a factor of 1.5) than those predicted by theory. These discrepancies are believed to arise from the DWBA analysis of the reaction mechanism. The inclusion of these effects into the calculation of the Re^{186} spectrum would result in an over-all increase in the predicted intensities with little or no change in their relative magnitudes.

Since the Re^{186} ground state has a cross section smaller than that which theory predicts, while the 320-keV doublet possesses a correspondingly larger cross section, the observed discrepancies could well be resolved by assuming the existence of a mixing between the ground-state rotational band and the $K^\pi = 1^-$ band at 316 keV. Theoretically, the Coriolis force cannot mix levels in these bands; however, the residual proton-neutron interaction can cause a mixing of the intrinsic configurations on which these bands are built. This interaction would have the gross effect of changing the entire character of each rotational band. Because little is known regarding the mixing of this type in odd-odd deformed nuclei, it is difficult to assess the degree of its importance in this particular case.

The calculation of reaction cross sections of low-lying levels in an odd-odd deformed nucleus provides a very severe test for the Nilsson wave functions employed. Ambiguities present in these wave functions could very easily go undetected in the study of odd-A nuclei and still cause serious discrepancies in neighboring odd-odd nuclei. Because Re^{186} is situated near the edge of the deformed region, the assumption that the nuclear motion can be separated into collective and intrinsic modes is certainly becoming less reliable. This in turn reduces the reliability of the "deformed" quasiparticle wave functions and implies that the band-

[49] V. G. Soloviev, Phys. Letters **21**, 320 (1966).
[50] A. Faessler, W. Greiner, and R. K. Sheline, Nucl. Phys. **70**, 33 (1965).
[51] R. H. Siemssen and J. R. Erskine, Phys. Rev. Letters **19**, 90 (1967).

mixing calculation presented here probably represents a combination of other effects. Within the framework of the Nilsson model, Coriolis mixing is a factor which must be considered; however, the question regarding the degree of its importance in the case of Re^{186} must await more refined experimental and theoretical studies.

IV. CONCLUSION

From the investigations presented in this work, it appears that the low-lying levels in Re^{186} can be qualitatively understood within the framework of the Nilsson model. Both configurations corresponding to the $K=\Omega_p+\Omega_n$ and $K=|\Omega_p-\Omega_n|$ coupling of the odd proton and neutron are indicated for the [402 ↑] and [512 ↓], the [402 ↑] and [510 ↑], and the [402 ↑] and [503 ↑] Nilsson states. The data also suggest that the 314-keV state may be an excited proton state corresponding to the p[514 ↑]; n[512 ↓] configuration.

Quantitatively, however, it appears that pure two-quasiparticle wave functions do not adequately represent even the low-lying levels in Re^{186}. This fact is particularly evident when one considers the charged-particle reaction cross sections. The inclusion of the effects due to the Coriolis interaction improves the agreement between the experimental and theoretical cross sections, but it does not adequately account for the intensity pattern exhibited by the ground-state rotational band. The fact that the proton-neutron residual interaction can mix the neutron configurations of the ground band and the $K^\pi=1^-$ band at 316 keV suggests that an explanation may lie in an extensive calculation of these mixing effects.

The correspondence of levels observed in the high-energy (n,γ) reaction with those observed in the (d,p) and (d,t) process is interesting. These data indicate that the $Re^{185}(n,\gamma)Re^{186}$ reaction—at least for lower-lying levels—appears to preferentially populate excited neutron configurations. This phenomenon has also been observed in the reactions $Ho^{165}(n,\gamma)Ho^{166}$ and $Tm^{169}(n,\gamma)Tm^{170}$.[52,53] Experimentally, it is known that the low-lying levels of both Ho^{166} and Tm^{170} generally result from the same neutron configurations. As a result, little could be inferred regarding the existence of a selective (n,γ) process which would tend to populate excited neutron configurations. The low-lying neutron configurations observed in Re^{186}, however, are different from those observed in Ho^{166} and Tm^{170}. The preferential population of excited neutron configurations in Re^{186}, therefore, suggests that this selection process may be quite general in deformed odd-odd nuclei.

Although the Re^{186} level scheme has been investigated through the (d,t) reaction, the full power of this method has not been utilized in these studies. It has not been possible to compare meaningfully the experimental and theoretical (d,t) intensities, because there are no reliable triton optical-model parameters available in this mass region. A DWBA analysis of the (d,t) reaction using triton optical-model parameters of Burke *et al.*[54] proved highly unreliable. In these investigations, therefore, the results of the (d,t) studies were limited to providing only qualitative comparisons with the (d,p) spectrum.

ACKNOWLEDGMENTS

We wish to thank Dr. Y. Shida for many invaluable and stimulating discussions during the preparation of this manuscript. We are grateful to Professor H. Maier-Leibnitz, Professor O. Kofoed-Hansen, Professor T. Bjerge, Dr. Fl. Juul, and Dr. H. T. Motz for their support of and continuous interest in this work. Thanks are also due to R. Maier for his kind assistance during the preparation of the target used in the (n,e^-) experiments at Risø; to Dr. T. Udagawa for providing us with the computer code for calculating reaction cross sections of two-quasiparticle states; to K. Chellis for his perserverence in fashioning the targets used in the (d,p) and (d,t) studies; to Professor K. O. Nilsson, who designed, and V. Toft, who assisted in a very important way in the installation of, the Florida State University isotope separator; and to Dr. J. Dawson, Dr. M. Minor, and D. Benson for their helpful assistance during the charged-particle reaction experiments. We are indebted to the staffs of the reactors: Omega West in Los Alamos, FRM near Munich, and DR-3 in Risø, and to the staff of the Florida State University tandem van de Graaff accelerator for their patient cooperation. The assistance of the personnel of the Leibniz Computing Center of the Bavarian Academy of Science and of the Florida State University CDC 6400 Computing Center is also gratefully acknowledged.

[52] H. T. Motz, E. T. Jurney, O. W. B. Schult, H. R. Koch, U. Gruber, B. P. Maier, H. Baader, G. L. Struble, J. Kern, R. K. Sheline, T. v. Egidy, Th. Elze, E. Bieber, and A. Bäcklin, Phys. Rev. **155**, 1265 (1967).

[53] R. K. Sheline, C. E. Watson, B. P. Maier, U. Gruber, R. H. Koch, O. W. B. Schult, H. T. Motz, E. T. Jurney, G. L. Struble, T. von Egidy, Th. Elze, and E. Bieber, Phys. Rev. **143**, 857 (1966).

[54] D. G. Burke, B. Zeidman, B. Elbek, B. Herskind, and M. Olesen, Kgl. Danske Videnskab. Selskab, Mat.-Fys. Medd. **35**, No. 2 (1966).